JBC RESEARCH ARTICLE

KAT8 is upregulated and recruited to the promoter of *Atg8* by FOXO to induce H4 acetylation for autophagy under 20-hydroxyecdysone regulation

Received for publication, October 16, 2023, and in revised form, January 11, 2024 Published, Papers in Press, February 1, 2024,
https://doi.org/10.1016/j.jbc.2024.105704

Tian-Wen Liu, Yu-Meng Zhao, Ke-Yan Jin, Jin-Xing Wang*, and Xiao-Fan Zhao*

From the Shandong Provincial Key Laboratory of Animal Cells and Developmental Biology, School of Life Sciences, Shandong University, Qingdao, China

Reviewed by members of the JBC Editorial Board. Edited by Brian D. Strahl

Selective gene expression in cells in physiological or pathological conditions is important for the growth and development of organisms. Acetylation of histone H4 at K16 (H4K16ac) catalyzed by histone acetyltransferase 8 (KAT8) is known to promote gene transcription; however, the regulation of KAT8 transcription and the mechanism by which KAT8 acetylates H4K16ac to promote specific gene expression are unclear. Using the lepidopteran insect *Helicoverpa armigera* as a model, we reveal that the transcription factor FOXO promotes KAT8 expression and recruits KAT8 to the promoter region of autophagy-related gene 8 (*Atg8*) to increase H4 acetylation at that location, enabling *Atg8* transcription under the steroid hormone 20-hydroxyecdysone (20E) regulation. H4K16ac levels are increased in the midgut during metamorphosis, which is consistent with the expression profiles of KAT8 and ATG8. Knockdown of *Kat8* using RNA interference results in delayed pupation and repression of midgut autophagy and decreases H4K16ac levels. Overexpression of KAT8-GFP promotes autophagy and increases H4K16ac levels. FOXO, KAT8, and H4K16ac colocalized at the FOXO-binding region to promote *Atg8* transcription under 20E regulation. Acetylated FOXO at K180 and K183 catalyzed by KAT8 promotes gene transcription for autophagy. 20E *via* FOXO promotes *Kat8* transcription. Knockdown or overexpression of FOXO appeared to give similar results as knockdown or overexpression of KAT8. Therefore, FOXO upregulates KAT8 expression and recruits KAT8 to the promoter region of *Atg8*, where the KAT8 induces H4 acetylation to promote *Atg8* transcription for autophagy under 20E regulation. This study reveals the mechanism that KAT8 promotes transcription of a specific gene.

Histone acetylation is a key mechanism to facilitate gene transcription. Histone acetylation is catalyzed by histone acetyltransferases (HATs), which transfer acetyl groups to the N-terminal lysine residue of a histone to neutralize its positive charge, thereby reducing its interaction with negatively charged DNA and leaving chromatin in an available state for transcription (1). HATs are divided into type A located in the nucleus and type B located in the cytoplasm. Type A includes three major families: MYST, P300/CBP, and GCNT (2). Histone acetyltransferase 8 (KAT8), also called MOF or MYST1, is a member of the MYST family with highly conserved functional domains and substrates from insect to human and is essential for the acetylation of histone H4 at K16 (H4K16ac) (3). Non-histone is also the substrate of KAT8, such as P53 (4). KAT8 is originally discovered in *Drosophila melanogaster* and is involved in forming the male-specific lethal complex and the nonspecific lethal complex (5). KAT8 plays important roles in a variety of life activities and functions specific to various cell and tissue types (6). KAT8 promotes the transcription of genes related to cell cycle progression and of genes related to autophagy (7). KAT8 and the level of H4K16ac act together as a molecular switch that regulates autophagy, in which the autophagic flux is increased while KAT8 is overexpressed (8). And the decrease of H4K16ac is associated with the downregulation of autophagy-related genes (9). However, the upstream transcription factor that regulates *Kat8* expression and how KAT8 specifically induces H4K16ac to enable gene transcription remain unclear.

The growth and development of insects are regulated by various hormones and the steroid hormone 20-hydroxyecdysone (20E) plays important role in the process. The 20E titer is low in feeding stage and is high during metamorphosis (10). 20E via its nuclear receptor (EcR) regulates the expression of metamorphic-related genes (11), such as transcription factor forkhead box O (FOXO), to promote metamorphosis (12). Insect larval cells undergo autophagy and apoptosis for tissue remodeling from larval to adult stages during metamorphosis, altering the external morphology and internal tissue structure. During metamorphosis, the larval midgut is disintegrated *via* forms of programmed cell death (13), including autophagy and apoptosis, and is replaced by newly formed imaginal tissues, a process regulated by 20E (14). In *Helicoverpa armigera*, autophagy and apoptosis occur in the larval midgut successively, and autophagy transforms into apoptosis under the regulation of 20E (15). The active form of ATG8 (autophagy-related gene 8; also named LC3, microtubule-associated protein one light chain 3-phosphatidylethanolamine) and cleaved caspase three only appear in the midgut at the metamorphic stages (15). The

* For correspondence: Xiao-Fan Zhao, xfzhao@sdu.edu.cn; Jin-Xing Wang, jxwang@sdu.edu.cn.

mechanism by which *Atg* genes are differentially expressed at different developmental stages is unclear.

The process of autophagy and the expression of *Atg* genes are tightly conserved and regulated by a variety of factors, such as specific transcription factors and epigenetic modifications (16, 17). FOXO promotes autophagy via upregulating the expression of *Atg* genes (*Atg1*, *Atg4*, *Atg8*, and *Atg14*) (18–20). The acetylation modification changes FOXO transcription activity (21). Previous studies have shown that prolonged oxidative stress leads to high acetylation of FOXO and promotes autophagy, which leads to cell death (22). *Atg* transcription is also regulated by histone modifications, such as the acetylation of H4K16 (23). KAT8 acetylates H4K16 (3, 24), and the acetylation of H4K16 leads to the expression of *Atg* genes for autophagy (25, 26). However, the relationship of FOXO, KAT8, and H4K16 acetylation are unclear.

We used the lepidopteran insect *H. armigera*, the cotton bollworm, as a model to investigate these questions. Our results showed that 20E via FOXO upregulated *Kat8* expression in the midgut during metamorphosis. KAT8 gave positive feedback to FOXO acetylation. FOXO recruited KAT8 to the promoter region of *Atg8* to acetylate H4K16 nearby, which promoted *Atg8* transcription for autophagy under 20E regulation.

Results

Screening of HATs highly expressed in midgut during metamorphosis

By BLAST assay, eight HATs were found in the *H. armigera* genome. Seven of them belong to class A (Fig. S1). Because class B HAT was localized in the cytoplasm, it has no effect on histone acetylation. So, the mRNA level of the seven HATs were examined in the epidermis, midgut, and fat body using quantitative real-time polymerase chain reaction (qRT-PCR) to screen the HAT highly expressed in midgut during metamorphosis. The results showed that *Kat6B* was highly expressed in fat body (Fig. S2*A*). *CBP* was highly expressed in epidermis (Fig. S2*B*). *Kat9*, *Kat2B*, and *Kat7* were highly expressed in epidermis and fat body (Fig. S2, *C–E*). *Kat8* and *Kat5* were lowly expressed in epidermis and highly expressed in midgut and fat body. Compared with the expression of *Kat5*, *Kat8* expression in the metamorphic period in midgut was significantly higher than that in the feeding stage. Meanwhile, the expression of *Kat8* was most consistent with that of *Atg8* (Fig. S2, *F–H*). To compare the gene expression in the midgut, we examined the mRNA levels of the above genes at different ages. The results showed that *Kat8* among the seven HATs had the highest expression level in the midgut and was consistent with the expression trend of *Atg8* (Fig. S2*I*). Thus, *Kat8* was chosen for further study.

H4K16ac increased, along with the increased KAT8 and ATG8 in the midgut during metamorphosis

To study the relationship of H4K16ac, KAT8, and ATG8, we performed Western blotting to observe their expression profiles in the midgut at different developmental stages. The results showed that KAT8 was highly expressed in the midgut during the metamorphic stage (MM). Meanwhile, ATG8-I and ATG8-II showed a significant increase in the midgut during metamorphosis (Fig. 1*A*). Higher levels of H4K16ac during metamorphosis were also detected compared with feeding stages (Fig. 1*B*). The specificity assays of all the antibodies were shown in supplementary figure 3 (Fig. S3). These data revealed that H4K16ac is upregulated and its expression profile is consistent with that of KAT8 and ATG8 during metamorphosis.

To determine KAT8 playing roles in the larval midgut or adult midgut, we detected its localization in the midgut using immunohistochemistry. The midgut at the sixth instar 96 h (6th-96 h)contained the inner larval midgut and the outer imaginal midgut, while the midgut at the sixth instar 24 h (6th-24 h) only contained larval midgut. KAT8 was mainly localized in the larval midgut of 6th-96 h larvae, a fewer in the adult midgut (Fig. 1*C*), which indicated that KAT8 has a vital role in the larval midgut during metamorphosis.

KAT8 promoted larval midgut autophagy by upregulating the H4K16ac level to promote Atg gene expression

To examine the function of KAT8 in larval midgut during metamorphosis, we injected *Kat8* dsRNA into sixth instar 6 h larvae to knock down *Kat8* expression. The pupation time was delayed for about 14 h after injection of *dsKat8* compared to larvae injected with dsRNA of fluorescence protein (*dsGFP*) (Fig. 1, *A* and *B*), with the efficiency of knockdown of *Kat8* confirmed by qRT-PCR and Western blot analysis (Fig. 1, *C* and *D*). Phenotype statistic analysis showed 52.4% of larvae were delayed in pupation time after *dsKat8* injection (Fig. 2*E*). Furthermore, the larval midgut of the control group turned red, an indication of midgut remodeling (27), but the ds*Kat8*-injected midgut did not turn red until 96 h after the first injection (Fig. 2*F*). HE staining showed that the separation of the larval midgut from the imaginal midgut was delayed after *dsKat8* injection compared with the control group (Fig. 2*G*). These data suggested that KAT8 is essential to midgut remodeling and pupation.

To study the mechanism of delayed midgut remodeling and pupation, we detected the H4K16ac level and the expression of *Atgs*. The acetylation level of H4K16 was decreased after *Kat8* knockdown (Fig. 2*H*). Western blotting showed that the active form of ATG8 (ATG8-II) were significantly reduced after *dsKat8* injection compared with the *dsGFP* control group (Fig. 2*I*). qRT-PCR showed that the mRNA level of *Atg1*, *-4*, *-7*, *-8*, and *-14* and the apoptosis-related gene *caspase3* were decreased after *Kat8* knockdown (Fig. 2*J*). These data suggested that *Kat8* promotes midgut autophagy and apoptosis by upregulating the expression of various *Atg* genes and *caspase3* and H4K16ac.

Overexpression of KAT8 promoted cell autophagy in HaEpi cells

To further verify the role of KAT8 in promoting autophagy, we overexpressed KAT8 fused with GFP in HaEpi cell line (the *H. armigera* epidermal cell line (28, 29)) (Fig. 3*A*). KAT8 was

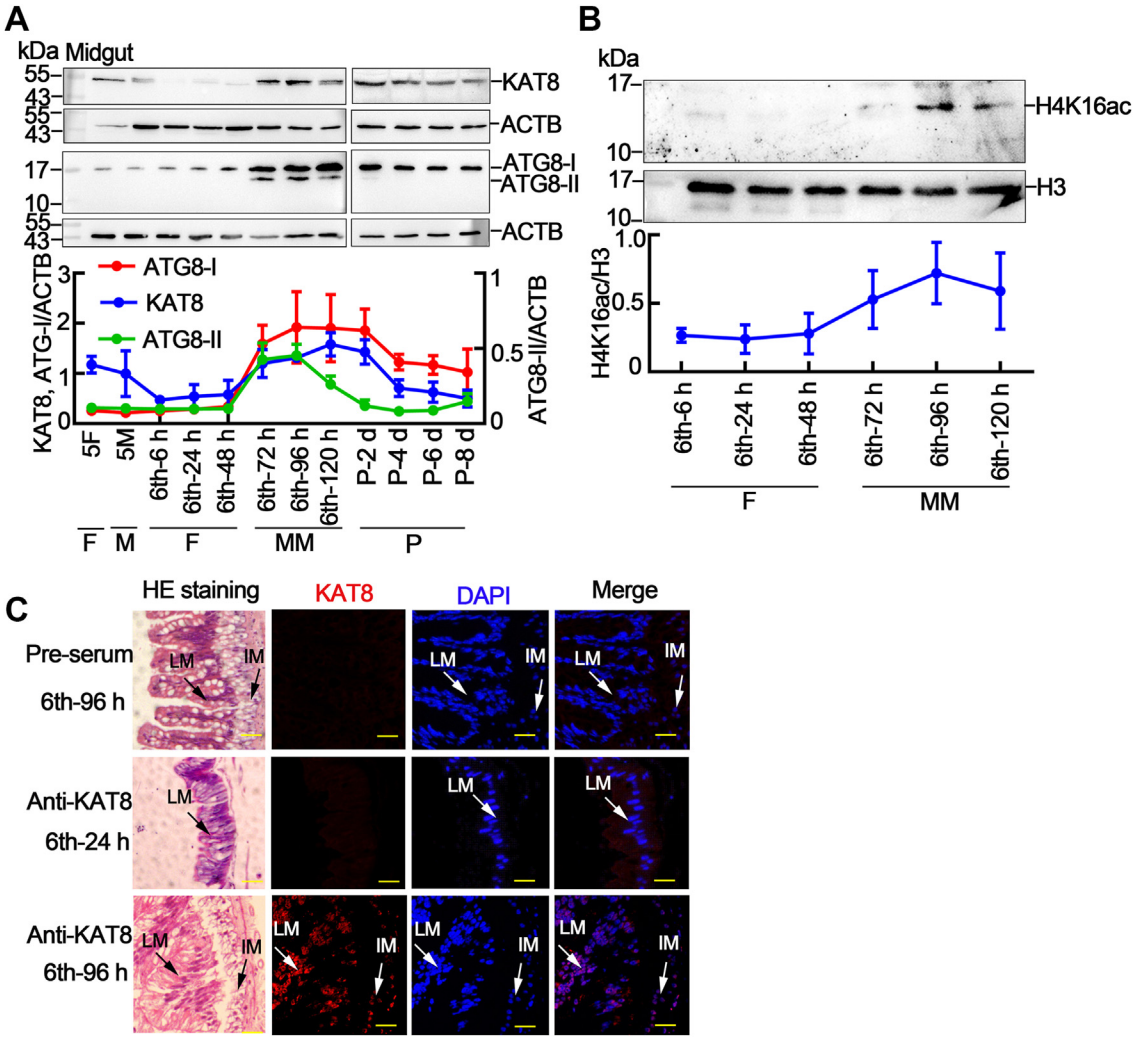

Figure 1. Western blot analysis of the expression of KAT8, ATG8, and H4K16ac. *A*, the protein expression levels and quantification of KAT8 and ATG8 in the midgut. ACTB was used as a protein loading control. 5F: 5th instar feeding larvae; 5 M: 5th instar molting larvae; 6th instar 6 h larvae to 6th instar 120 h larvae; P-2 d to P-8 d: pupal stage at day 2 to day 8; F: feeding stage; M: molting stage; MM: metamorphic molting stage; P: pupae. The data were quantified according to three independent replicates using ImageJ software. *B*, the levels of H4K16ac in the midgut. Histone H3 was used as a protein quantity control. 6th-6 h to 6th-120 h: 6th instar 6 h larvae to 6th instar 120 h larvae; F: feeding stage; M: molting stage; MM: metamorphic molting stage. *C*, the location of KAT8 detected with immunohistochemistry. HE staining showing the morphology of the midgut. *Red*, KAT8 detected using anti-KAT8 antibodies; *blue*, nuclei stained using DAPI. Bar represents 20 μm. Images of HE staining and immunofluorescence are from two adjacent slices. The statistical analysis was performed using Student's *t* test (*$p < 0.05$, **$p < 0.01$, ***$p < 0.001$, n = 3). The error bar indicates the mean ± S.D. H4K16ac, acetylation of histone H4 at K16; IM, imaginal midgut; LM, larval midgut.

localized in the nucleus and its location was not altered by 20E treatment (Fig. 3*B*). The mRNA level of *Atg8* was increased after overexpression of KAT8-GFP was compared to the overexpression of GFP (Fig. 3*C*). Western blot analysis showed that KAT8 increased ATG8 expression (Fig. 3*D*). The level of H4K16ac was also increased after overexpressed KAT8 (Fig. 3*E*). The role of KAT8 on autophagy was further verified by cotransfected His or KAT8-His (without GFP) and a pIEx-4-RFP-GFP-LC3-His reporter plasmid in HaEpi cells together for 72 h. After cells were inducted with 5 μM 20E for 6 h, autophagic vacuoles appeared in cells compared with dimethyl sulfoxide (DMSO) group. 3-Methyladenine, an autophagy inhibitor, inhibited autophagy. Compared with the control overexpressing His tag, overexpression of KAT8-His accelerated the process of autophagic flux, as indicated by the decrease of autophagosome and GFP fluorescence quenching, but increased autolysosome number (Fig. 3, *F* and *Fi*), as GFP fluorescence quenching by the acidic pH in the autolysosomes indicated autophagic flux from autophagosome to autolysosome (30). These data further confirmed that KAT8 induces cell autophagy.

FOXO recruited KAT8 binding to the promoter region of Atg8

FOXO promotes autophagy by promoting ATG expression (31), so we addressed the relationship among FOXO, KAT8, and H4K16ac by co-immunoprecipitation (Co-IP) in midgut and in HaEpi cells. FOXO was co-immunoprecipitated with H4K16ac and KAT8 using anti-KAT8 antibodies in the 6th-96 h midgut after normalizing the nuclear proteins by H3 and actin (Fig. 4*A*), suggesting that FOXO, H4K16ac, and KAT8 interacted in the 6th-96 h midgut.

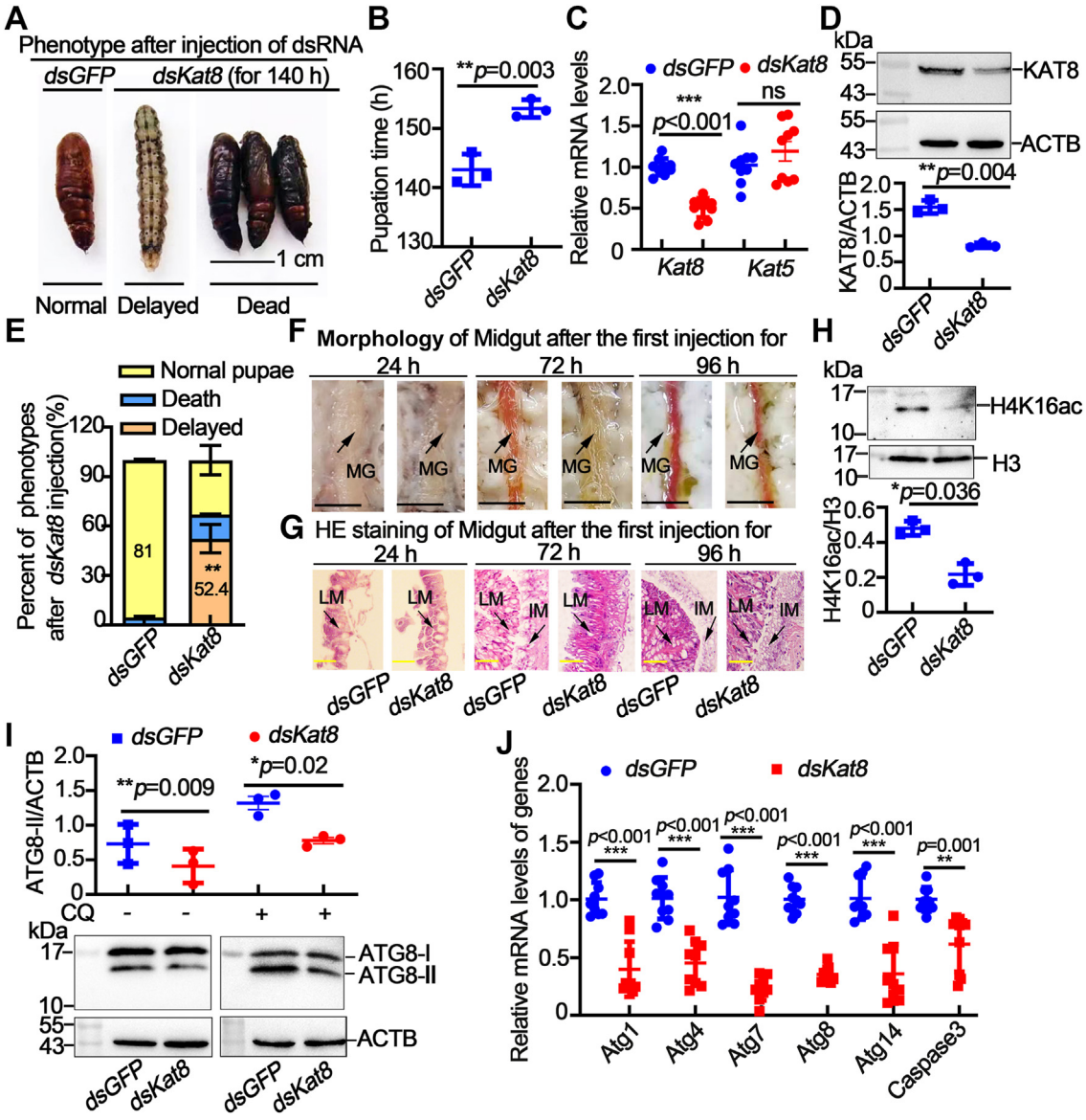

Figure 2. Knockdown of *Kat8* delayed larval-pupal transition and suppressed *Atg* gene expression. *A*, the phenotypes after *dsGFP* or ds*Kat8* injection 24 h after the third injection (2 μg/larva). *B*, statistical analysis of the pupation time. n = 30/group and repeat three times. *C*, efficiency of the knockdown of *Kat8* by qRT-PCR analysis, *Kat5* was used as the off-target assay. *D*, efficiency of the knockdown of *Kat8* by Western blot analysis. *E*, the statistical analysis of the percentage of different phenotypes after the *dsGFP* or *dsKat8* injection. Each group contained 30 larvae. The data were analyzed using three independent replicates by Student's *t* test. *F*, the morphology of the midgut after the dsRNA injection. The scale bar represented 0.5 cm. *G*, HE staining of the midgut 24 h and 48 h after the last dsRNA injection. Scale bar represents 20 μm. *H*, Western blot and statistical analysis of the level of H4K16ac after dsRNA injection. *I*, Western blot and statistical analysis of the expression of ATG8-II after dsRNA injection. *J*, qRT-PCR shows the expression of *Atg* genes and *caspase3*. The statistical analysis was performed using Student's *t* test (*$p < 0.05$, **$p < 0.01$, ***$p < 0.001$, n = 3). The error bar indicates the mean ± S.D. ATG8, autophagy-related gene 8; H4K16ac, acetylation of histone H4 at K16; IM, imaginal midgut; LM, larval midgut; qRT-PCR, quantitative real-time polymerase chain reaction.

KAT8-GFP and FOXO-RFP were then co-transfected in HaEpi cells and Co-IP assay was performed after treatment with 20E or DMSO to further study the interaction of the proteins. The overexpressed FOXO-RFP was localized in the nucleus (Fig. S4). KAT8-GFP, FOXO-RFP, and H4K16ac were coprecipitated by an anti-GFP antibody that immunoprecipitated KAT8-GFP, which the interaction was significantly increased by 20E induction, compared with DMSO treatment (Fig. 4*B*). Meanwhile, an *in vitro* GST-Pull down assay was carried out and the results showed that FOXO-GST pulled down KAT8-GFP from cell lysate overexpressed with KAT8-GFP (Fig. S5). These data confirmed that KAT8-GFP, FOXO-RFP, and H4K16ac interact with each other, and the interaction is increased by 20E.

A chromatin immunoprecipitation (ChIP) assay was performed to confirm the colocation of the proteins in the same DNA site in the promoter of *Atg8*. The FOXO-binding element (FOXOBE) was predicted in the promoters of *Atg* genes, including *Atg1*, *Atg4*, *Atg8*, and *Atg14* (Fig. S6). Two possible FOXO-binding sites (-589AGTTTAT-581 and -546ATATAAACA-537) were predicted in the *Atg8* promoter which were similar to the conserved FOXOBE: TTGTTTAT or (T/C)(G/A)AAACAA (32, 33). The ChIP assay showed that FOXO-GFP can bind to the two FOXOBE-contained

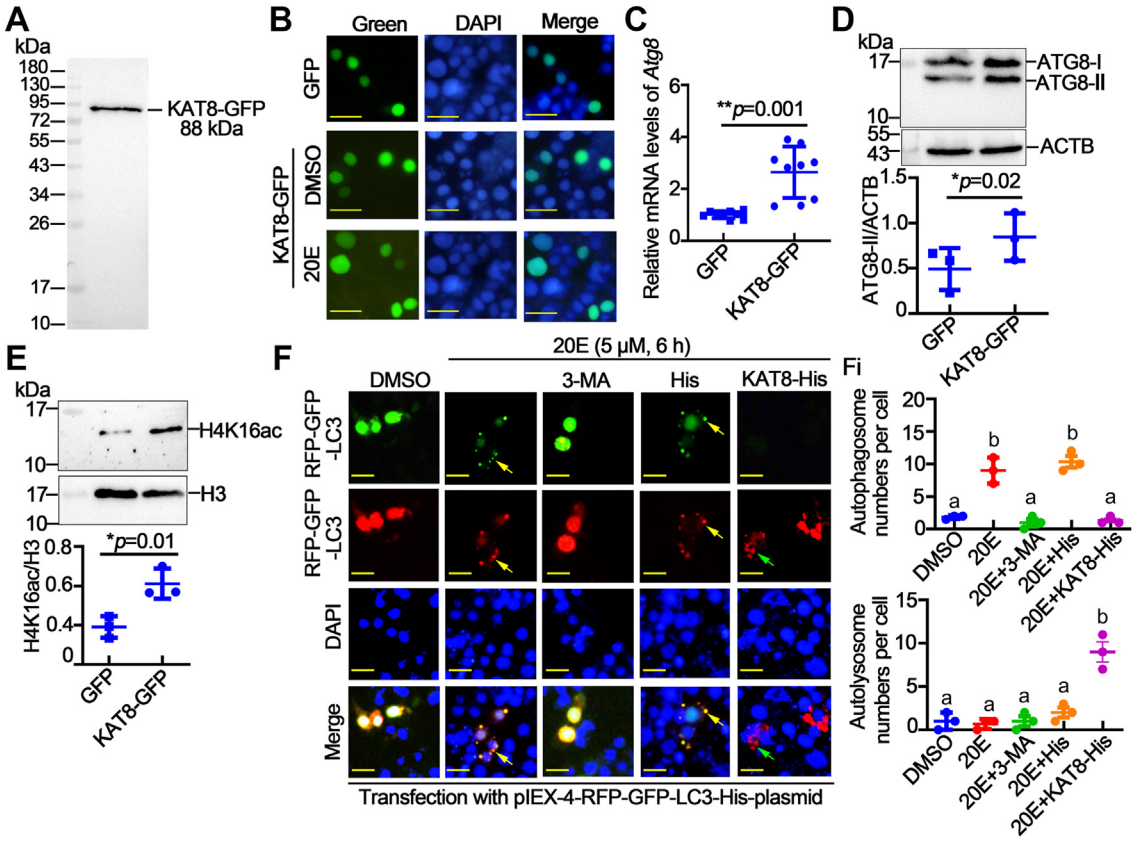

Figure 3. Overexpression of KAT8 in HaEpi cells induced autophagy. *A*, Western blot analysis showing GFP and KAT8-GFP levels in HaEpi cells 72 h after transfection. *B*, subcellular localization of KAT8-GFP after 72 h of overexpression. *Blue*, nucleus stained with DAPI; *green*, KAT8-GFP. Bar represents 20 μm. *C*, the mRNA level of *Atg8* with overexpression of GFP and KAT8-GFP in cells. *D*, Western blot analysis showing the bands for ATG8-I and ATG8-II with the overexpression of GFP and KAT8-GFP in HaEpi cells. *E*, Western blotting showing the band for H4K16ac with overexpression of GFP and KAT8-GFP in HaEpi cells. *F*, autolysosomes were detected after His or KAT8-His, and pIEx-4-RFP-GFP-LC3-His were overexpressed in HaEpi cells for 72 h. The *yellow* arrows represent autophagosomes and the *green* arrows represent autolysosomes. Bar represents 20 μm. *Fi*, the number of autophagosomes and autolysosome puncta per cell transfected successfully from per total of about 50 cells. The statistical analysis was performed using Student's *t* test (*$p < 0.05$, **$p < 0.01$, ***$p < 0.001$, n = 3) and Anova. The error bar indicates the mean ± S.D. ATG8, autophagy-related gene 8; H4K16ac, acetylation of histone H4 at K16; HaEpi, *H. armigera* epidermal cell line.

fragments in the promoter of *Atg8* and the amount was increased with 20E induction than with DMSO treatment, compared with IgG as an antibody control and primer *Atg8* as nonspecific DNA-binding control (Fig. 4*C*). These results suggested that FOXO bound the FOXOBE of *Atg8*.

To address the colocalization of KAT8-GFP and H4K16ac on the two FOXOBE-contained fragments in the promoter of *Atg8*, ChIP assays were performed with antibody against GFP that recognized the overexpressed KAT8-GFP and antibodies against H4K16ac that recognized the acetylated H4K16, respectively. The results showed that antibody against GFP and antibodies against H4K16ac showed enriched KAT8-GFP and H4K16ac, respectively, on the FOXOBE-containing sequence under 20E induction, compared with the DMSO and primer *Atg8* controls (Fig. 4, *D* and *E*). These data suggested that FOXO, KAT8, and H4K16ac are colocalized in the promoter region of *Atg8*, and KAT8 is recruited to the binding region by FOXO and then acetylate H4K16 to promote *Atg* genes transcription.

It has been reported that KAT8 catalyzes H4K5ac and H4K8ac in the promoter region to promote gene transcription (34). To determine the enrichment of H4K5ac and H4K8ac on the FOXO-binding region, we performed ChIP assays with antibodies against H4K5ac and H4K8ac, respectively. The specificity of the antibodies was verified by Western blot (Fig. S7*A*). The results showed that the FOXOBE fragment amount was increased with 20E induction than with DMSO treatment, compared with IgG as an antibody control and primer *Atg8* as nonspecific DNA-binding control (Fig. S7, *B* and *C*). This suggested that KAT8 also mediates the acetylation of H4K5 and H4K8 in the promoter region of *Atg8* to promote *Atg8* transcription.

20E induced FOXO acetylation via KAT8

To further determine the interaction between FOXO and KAT8, we examined the expression profile of FOXO during development from feeding to metamorphosis. FOXO was highly expressed during metamorphosis (Fig. 5*A*). The acetylation of FOXO in 6th-96 h wandering larvae was increased compared to the 6th-24 h feeding larvae when the FOXO loading levels were normalized (Fig. 5*B*). FOXO acetylation level was increased and its location was shifted from the cytoplasm to the nucleus with 20E stimulation (Fig. 5, *C* and *D*). FOXO was nonacetylated in the cytoplasm during feeding stage (6th-24 h), and FOXO was

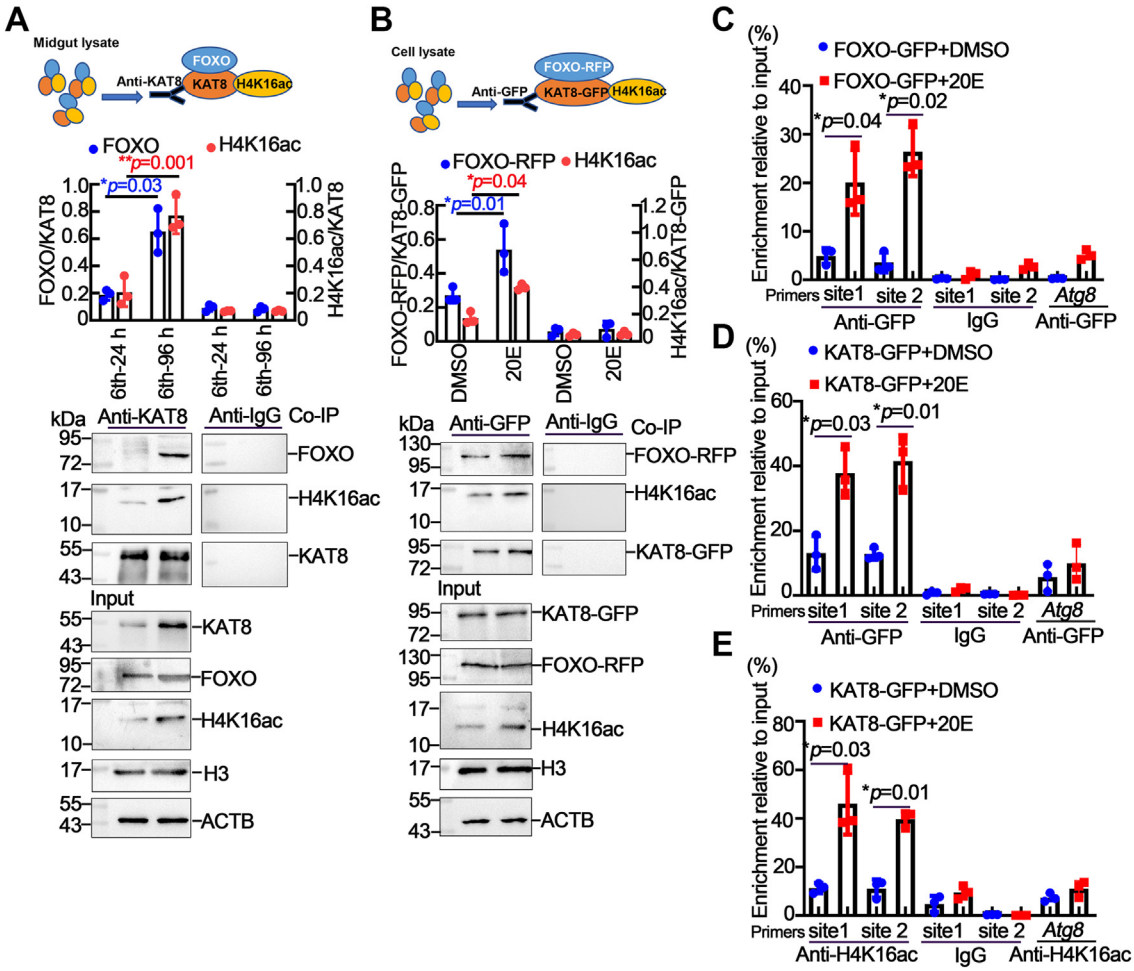

Figure 4. 20E increased the interaction between KAT8, H4K16ac, and FOXO and colocalization in the promoter regions of *Atg8*. *A*, Co-IP assay in 6th-24 h and 6th-96 h midgut. Anti-KAT8 antibodies co-immunoprecipitated KAT8, FOXO, and H4K16ac and then were detected using anti-KAT8 antibodies, anti-FOXO antibodies, and H4K16ac antibodies, respectively. Rabbit IgG (IgG) was used as a negative control. *B*, Co-IP assay in HaEpi cells. KAT8-GFP and FOXO-RFP were overexpressed in HaEpi cells and incubated with 5 μM 20E for 6 h, with an equal amount of DMSO used as a control. Anti-GFP antibody co-immunoprecipitated KAT8-GFP, FOXO-RFP, and H4K16ac and then were detected using anti-GFP antibody, anti-RFP antibody, and H4K16ac antibodies, respectively. Rabbit or mouse IgG (IgG) was used as a negative control. *C*, ChIP assay of FOXO-GFP at the *Atg8* promoter region with antibody against GFP using different primers (Table S1). *D* and *E*, ChIP assay of KAT8-GFP and H4K16ac at the promoter region of *Atg8* with antibodies against GFP and H4K16ac using different primers (Table S1), respectively. Input: nonimmunoprecipitated chromatin. IgG, nonspecific mouse or rabbit IgG. Primer site1 and site2 were the sequence containing FOXOBE. Primer *Atg8* was targeted to the *Atg8* ORF. The statistical analysis was performed using Student's *t* test (*$p < 0.05$, **$p < 0.01$, ***$p < 0.001$, n = 3 repeats/group). The error bar indicates the mean ± S.D. ATG8, autophagy-related gene 8; Co-IP, co-immunoprecipitation; DMSO, dimethyl sulfoxide; FOXO, forkhead box O; FOXOBE, FOXO-binding element; H4K16ac, acetylation of histone H4 at K16; HaEpi, *H. armigera* epidermal cell line.

acetylated in nucleus during metamorphic stage (sixth-96 h) (Fig. 5*E*). These results revealed that 20E induces FOXO acetylation and nuclear location.

We found that KAT8 can acetylate FOXO by predicting on the website (http://pail.biocuckoo.org/wsresult.php). To examine the possibility that KAT8 acetylating FOXO, *Kat8* was knocked down *in vivo* by RNAi and overexpression in HaEpi cells. Results showed that the acetylation of FOXO was significantly decreased after *Kat8* knockdown (Fig. 5*F*). In contrast, the acetylation of FOXO was increased after overexpression of KAT8-GFP in HaEpi cells with 6 h treatment of 20E (Fig. 5*G*). Meanwhile, we performed *in vitro* acetylation assay by incubating recombinant FOXO-GST purified from *Escherichia coli* with KAT8-GFP immunoprecipitated from HaEpi cells. A strong acetylation of FOXO-GST was observed with the presence of acetyl-CoA (Fig. 5*H*). These results indicated that KAT8 acetylates FOXO directly.

We further explored the acetylation sites of FOXO by predicting on the website (http://pail.biocuckoo.org/online.php) as a reference for FOXO site-directed mutagenesis. The lysine at position 169 (score 4.9), lysine at position 180 (score 7.6), and lysine at 183 (score 4.1) were predicted to be the possible acetylation sites catalyzed by KAT8. Meanwhile, we found that the three lysine sites were conserved with human and mouse by performing sequence alignment (Fig. S8). We constructed mutant plasmids with arginine instead of lysine to study their contribution to FOXO acetylation. WT FOXO showed high level of acetylation under 20E induction. The three mutants showed significantly lower level of acetylation. Among them, K180R-FOXO showed the lowest level of acetylation (Fig. 6*A*). All three mutants were localized in the nucleus, indicating that acetylation of these three sites did not affect the nuclear localization of FOXO-GFP (Fig. 6*B*). We overexpressed WT FOXO and FOXO mutants in HaEpi cells to explore the

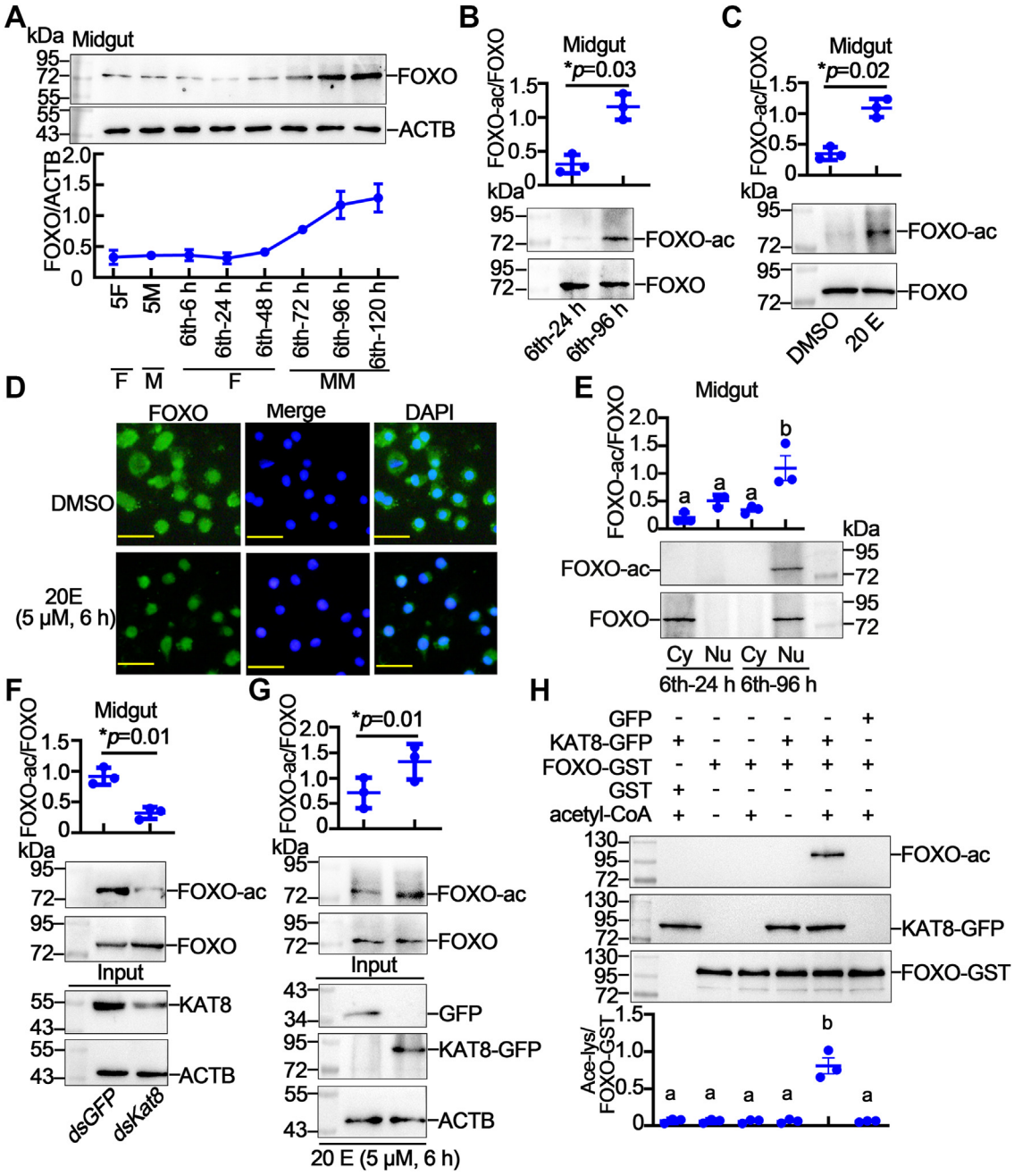

Figure 5. 20E promoted FOXO acetylation through KAT8. *A*, the expression profiles of FOXO in the midgut. *B*, the levels of FOXO acetylation in 6th-24 h and 6th-96 h midgut. *C*, the levels of FOXO acetylation in midgut after DMSO and 20E (5 μM, 6 h) treatment. *D*, the location of FOXO in HaEpi cells after DMSO and 20E treatment. *Blue*, nucleus stained with DAPI; *green*, FOXO. Bar represents 20 μm. *E*, Western blot analysis showing the subcellular distribution of acetylated and nonacetylated FoxO in the midgut at different developmental stages. *F*, the levels of FOXO acetylation after *dsKat8* injection for 72 h. *G*, the levels of FOXO acetylation in HaEpi cells overexpressing GFP and KAT8-GFP under 20E treatment (5 μM, 6 h). *H*, *in vitro* FOXO acetylation assay. Purified soluble FOXO-GST from *E. coli* was incubated with KAT8-GFP immunoprecipitated from HaEpi cells, in the presence or absence of acetyl-CoA. Anti-acetyl lysine antibodies were used to analyze FOXO acetylation by Western blot. The statistical analysis was performed using Student's *t* test (*$p < 0.05$, **$p < 0.01$, ***$p < 0.001$, n = 3). Statistical analysis of (*E*) and (*H*) was conducted using Anova; different letters represented significant differences ($p < 0.05$). The error bar indicates the mean ± S.D. DMSO, dimethyl sulfoxide; FOXO, forkhead box O; HaEpi, *H. armigera* epidermal cell line.

function of FOXO acetylation. The results showed an increase in ATG8-II in the overexpressed WT FOXO and K169R-GFP compared to the overexpressed GFP group, whereas there was no significant change in ATG8-II in the overexpressed K180R-GFP and K183R-GFP. (Fig. 6*C*). Meanwhile qRT-PCR showed that K180R-GFP and K183R-GFP impaired the ability of FOXO to promote the transcription of *Kat8*, *Atg8*, and *Caspase3* (Fig. 6*D*). The acetylation at K169 had no effect on the autophagy promotion of FOXO. However, it cannot be excluded that it will have a role in other functions of FOXO.

To further explain the function of acetylation in promoting the transcriptional activity of FOXO, we performed ChIP assays to verify the binding ability of different mutants to chromatin. The results showed that mutants enriched fewer

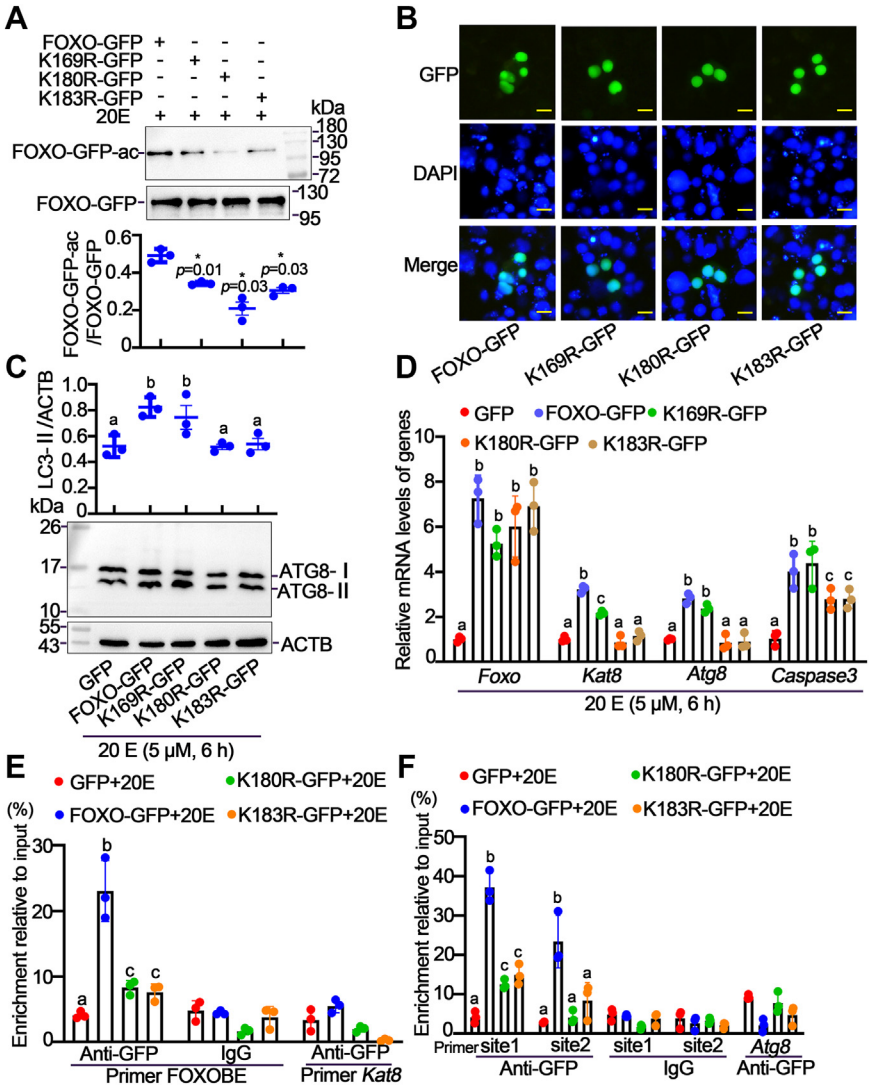

Figure 6. Acetylated FOXO promoted gene transcription for autophagy. *A*, site mutation to analyze lysine acetylation of FOXO. Student's *t* test (*$p < 0.05$, **$p < 0.01$, ***$p < 0.001$, n = 3). *B*, the subcellular localization of FOXO-GFP of the three mutants in the HaEpi cells. *Blue*, nucleus stained with DAPI; *green* represents FOXO-GFP, K169R-GFP, K180R-GFP, and K183R-GFP. Bar represents 20 μm. *C*, Western blotting and statistical analysis of the expression of ATG8-II after transfected with GFP, FOXO-GFP, and the three mutants. *D*, qRT-PCR detected the genes expression in HaEpi cells overexpressing GFP, FOXO-GFP, and three mutants. *E*, an anti-GFP antibody was used to immunoprecipitate FOXOBE containing fragment in the *Kat8* promoter region. Input: non-immunoprecipitated chromatin. IgG, nonspecific mouse IgG. Primer FOXOBE was the sequence containing FOXOBE. Primer *Kat8* was targeted to *Kat8* ORF. *F*, an anti-GFP antibody was used to immunoprecipitate FOXOBE containing fragment in the *Atg8* promoter region. Input: nonimmunoprecipitated chromatin. IgG, nonspecific mouse IgG. Primer site1,2 were the sequence containing FOXOBE. Primer *Atg8* was targeted to *Atg8* ORF. Statistical analysis of (*B–F*) was conducted using Anova; different letters represented significant differences ($p < 0.05$). The error bar indicates the mean ± S.D. FOXO, forkhead box O; qRT-PCR, quantitative real-time polymerase chain reaction; ATG8, autophagy-related gene 8; HaEpi, *H. armigera* epidermal cell line; FOXOBE, FOXO-binding element;

FOXOBE-containing DNA fragments than wild FOXO-GFP under 20E regulation (Fig. 6, *E* and *F*). These data suggested that acetylation modification at K180 and K183 is crucial for the function of FOXO in promoting *Atg8* transcription for autophagy.

20E through FOXO upregulated Kat8 *expression*

To analyze the regulation of 20E on the expression of *Kat8*, 20E (100–500 ng) was injected into sixth instar 6 h larval hemocoel for 6 h. The mRNA level of *Kat8* increased after 20E injections, compared with the treatment of DMSO in the midgut (Fig. 7*A*). Furthermore, 500 ng of 20E upregulated *Kat8* expression from 6 to 12 h in the midgut (Fig. 7*B*). These data suggested that 20E promotes *Kat8* expression in the midgut.

To further verify the mechanism by which 20E regulated *Kat8*, the promoter sequence of *Kat8* was analyzed to find the binding sites of transcription factors. A FOXOBE was found in the promoter region of *Kat8* using the JASPAR website (http://jaspar.genereg.net/), (5'-527-GTGTTTAT-519-3'), which was conserved with the FOXOBE sequence (5'-50-TTGTTTAC-30-3') in the promoter region of *H. armigera Brz7* (12). To investigate whether 20E promotes KAT8 transcription through FOXO, we injected *dsFoxo* to knock down *Foxo* expression. The results showed a decreased expression of *Kat8* after

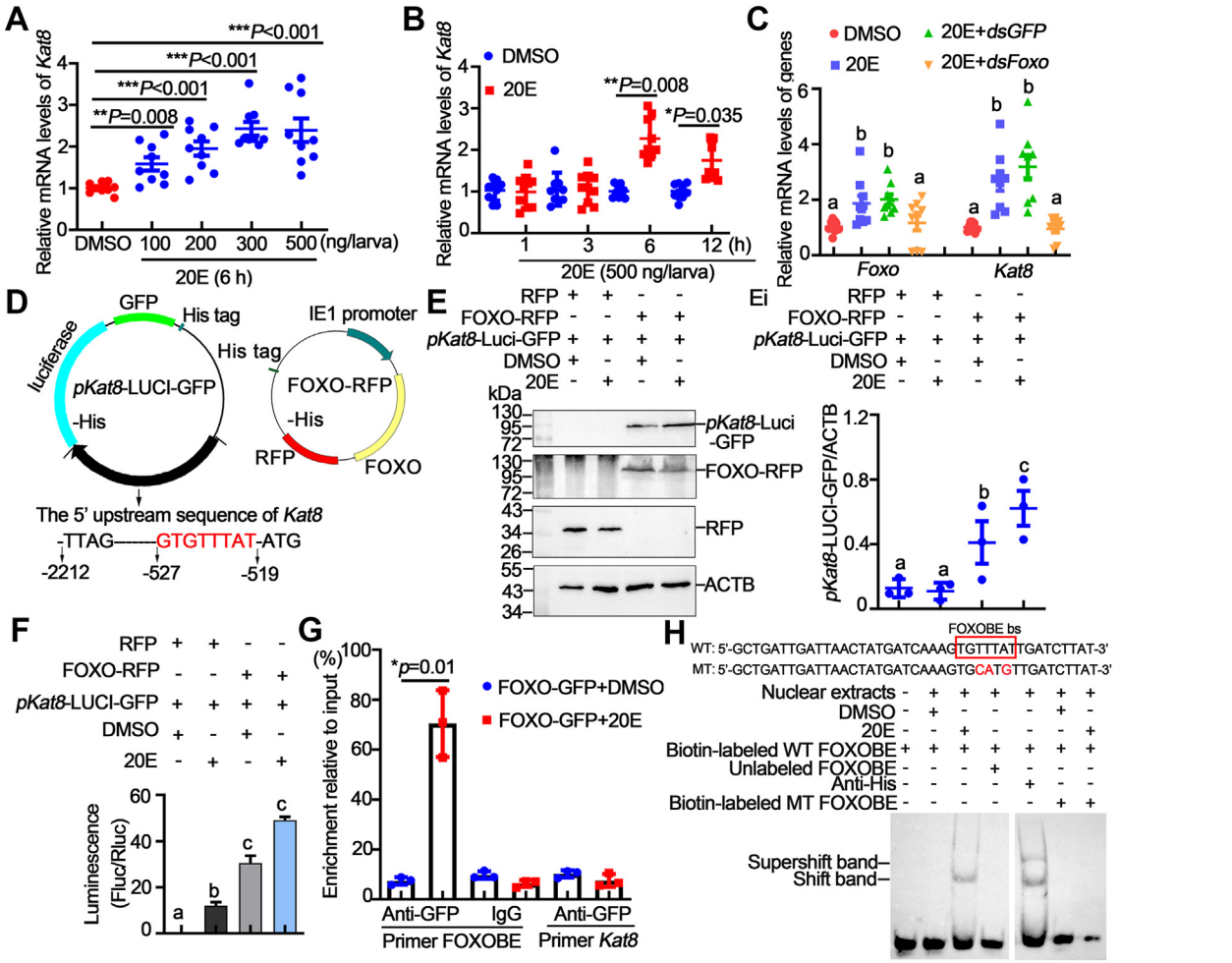

Figure 7. 20E *via* FOXO increased the expression of *Kat8*. *A*, the mRNA levels of *Kat8* in the midgut 6 h after 20E was injected into sixth instar 6 h larvae. An equal diluted volume of DMSO (0–500 ng) was used as the solvent control. *B*, the mRNA levels of *Kat8* in the midgut 1 to 12 h after 20E was injected into sixth instar 6 h larvae. *C*, 2 μg *dsFoxo* was injected into sixth instar 6 h larvae followed by stimulation with 20E for 12 h to detect the mRNA levels of *Kat8*. An equal diluted amount of DMSO was used as a control. *D*, plasmid maps of *pKat8*-LUCI-GFP-His and FOXO-RFP. *E*, Western blot analysis showing the expression of LUCI-GFP. *Ei*, the statistical analysis of (*E*). *F*, transcriptional activity assays. The RLU value of the firefly luciferase assay divided by the RLU value of the Renilla luciferase assay was the activity. *G*, ChIP analysis of FOXO binding to the *Kat8* promoter region. Input: nonimmunoprecipitated chromatin. IgG, nonspecific mouse IgG. Primer FOXOBE was the sequence containing FOXOBE. Primer *Kat8* was targeted to the *Kat8* ORF. *H*, FOXOBE on the *Kat8* promoter region bound to FOXO detected by EMSA assay. WT and MT represent FOXOBE probe and FOXBE mutant probe, respectively. The statistical analysis was performed using Student's *t* test (*$p < 0.05$, **$p < 0.01$, ***$p < 0.001$, n = 3). Statistical analysis of (*C*), (*E*), and (*F*) was conducted using Anova; different letters represented significant differences ($p < 0.05$). The error bar indicates the mean ± S.D. DMSO, dimethyl sulfoxide; FOXO, forkhead box O; FOXOBE, FOXO-binding element; RLU, relative light unit.

knockdown of *Foxo* (Fig. 7*C*), suggesting that FOXO is necessary for *Kat8* transcription.

The 5′ upstream sequence containing the binding region was replaced in the pIEx-4-luciferase-GFP-His plasmid to construct the reporter plasmid *pKat8*-LUCI-GFP-His (Fig. 7*D*) and was cotransfected with the FOXO-RFP-His overexpression plasmid in HaEpi cells to assess the regulation of FOXO on *Kat8*. Western blotting showed that the expression of LUCI-GFP was increased in FOXO-RFP-His overexpressing cells, whereas LUCI-GFP was not expressed in the RFP control (Fig. 7, *E* and *Ei*). Luciferase activity assays confirmed that FOXO enhanced the transcriptional activity of *Kat8*, which was enhanced by 20E addition (Fig. 7*F*). These data suggested that 20E via FOXO promotes *Kat8* transcription.

ChIP assay was used to further analyze the binding of FOXO to the FOXOBE of *Kat8*. FOXO-GFP binding to FOXOBEs increased with 20E induction compared with DMSO treatment (Fig. 7*G*). Given that FOXO formed a transcriptional complex with KAT8 to promote *Atg8* transcription, we speculated FOXO recruited KAT8 in the *Kat8* promoter as it does in the *Atg8* promoter. Therefore, we overexpressed KAT8-GFP in HaEpi cells for 72 h and performed ChIP assay with anti-GFP antibody and anti-H4K16ac antibodies, respectively. The results showed that more FOXOBE-containing DNA fragment was detected in 20E-induced cells than in DMSO treatment (Fig. S9, *A* and *B*), suggesting transcriptional complex consisted with FOXO and KAT8 promote gene transcription. Meanwhile, a biotin-labeled probe containing FOXOBE sequence was used for EMSA. DNA probe was combined by the nuclear protein extracts overexpressing FOXO-GFP-His with 20E treatment and a super shift band appeared with antibody against His-tag. And the mutated probe was not able

to be combined by the nuclear protein extracts (Fig. 7*H*). These results suggested that FOXO upregulates *Kat8* expression by binding to the FOXOBE motif in the promoter of *Kat8* under 20E regulation.

FOXO promoted midgut autophagy by upregulating the KAT8 expression to promote Atg *gene expression*

The dsRNA of *Foxo* was injected into sixth instar 6 h larvae to knock down *Foxo* expression to examine the regulation of FOXO on KAT8, H4K16ac, ATG8, and autophagy *in vivo*. The pupation was delayed after *dsFoxo* injection (Fig. 8*A*). The interference efficiency was confirmed using Western blot (Fig. 8*B*). 45.0% of the larvae delayed pupation by about 19 h after *dsFoxo* injection (Fig. 8, *C* and *D*). The midgut in the control group appeared red at 72 h post the first *dsGFP* injection, which was a character of programmed cell death, whereas the midgut did not appear red until 96 h after *dsFoxo* injection. HE staining showed the larval midgut and imaginal midgut was separated in the control group after *dsGFP* injection for 72 h, but the separation occurred at 96 h post the *dsFoxo* injection (Fig. 8*E*). Western blotting showed a decrease in KAT8 protein level after *Foxo* knockdown (Fig. 8*F*). Meanwhile, the acetylation levels of H4K16 and ATG8-II were significantly decreased (Fig. 8, *G* and *H*). In contrast, overexpression of FOXO in HaEpi cells caused the increase of KAT8, H4K16ac, and the level of ATG8-I and ATG-II (Fig. S10, *A*–*C*). These data suggested that FOXO upregulates KAT8 expression, which in turn increases the expression of ATG8 and H4k16ac, thereby promoting autophagy.

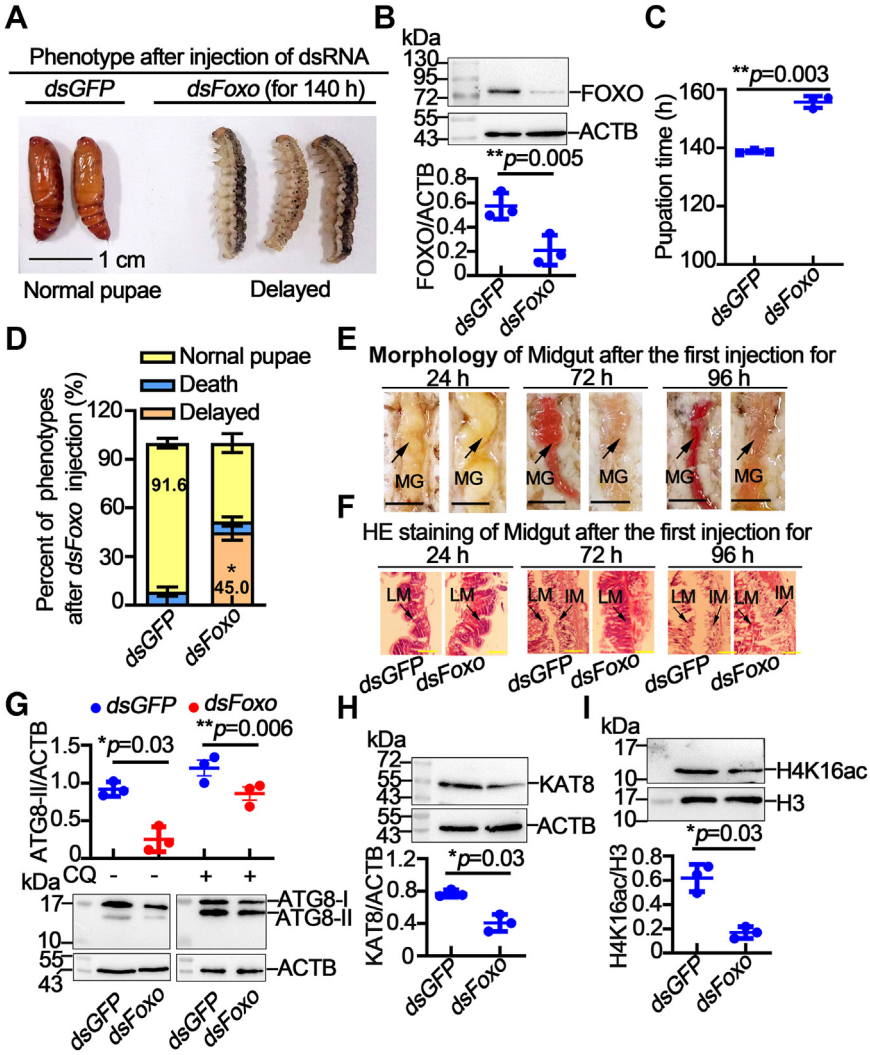

Figure 8. Knockdown of *Foxo* delayed larval-pupal transition. *A*, the phenotypes after *Foxo* knockdown 24 h after the third injection (2 μg/larva). *B*, efficiency of the knockdown of *Foxo* by Western blot analysis. *C*, statistical analysis of the pupation time. n = 30/group and repeat three times. *D*, the statistical analysis of the percentage of different phenotypes after the *dsGFP* or *dsFoxo* injection. Each group contained 30 larvae. The data were analyzed using three independent replicates by Student's *t* test. *E*, the morphology of the midgut at 24 h, 72 h, and 96 h after the first injection. The scale bar represented 0.5 cm. *F*, HE staining of the midgut at 24 h and 48 h after the first *dsRNA* injection. Scale bar represents 20 μm. *G*, Western blotting and statistical analysis of KAT8 expression 24 h after the third injection. *H*, Western blotting and statistical analysis of the expression of ATG8-II after the *dsRNA* injection. *I*, Western blotting and statistical analysis of the level of H4K16ac after *dsRNA* injection. The statistical analysis was performed using Student's *t* test (*$p < 0.05$, **$p < 0.01$, *** $p < 0.001$, n = 3 repeats/group). The error bar indicates the mean ± S.D. ATG8, autophagy-related gene 8; FOXO, forkhead box O; H4K16ac, acetylation of histone H4 at K16; IM, imaginal midgut; LM, larval midgut.

Discussion

KAT8 has important functions for gene expression by acetylating H4K16 to open the DNA strand, but how KAT8 specifically acetylates H4K16 in DNA for a gene transcription and its upstream regulator were unclear until now. This study revealed that the steroid hormone 20E upregulated KAT8 transcription via FOXO. KAT8 acetylated FOXO in a feedback way. KAT8-mediated acetylation increased transcriptional activity of FOXO. FOXO recruited KAT8 to FOXO binding region in the promoter of *Atg8*, where KAT8 induced the acetylation of H4K16 to open the DNA for the transcription of *Atg8* for autophagy.

KAT8 promoted larval midgut autophagy during insect midgut remodeling

KAT8 plays a vital role in determining the life and death of cells and organism (35), inducing apoptosis by acetylating non-histone P53 in humans (4) and in *D. melanogaster* (36) and promoting autophagosome-lysosome fusion (37). KAT8 overexpression increases autophagic flux in humans (9, 17). Low expression of KAT8, always accompanied by a decrease in H4K16ac, is considered a common marker in many cancers, such as ovarian, breast, gastric, prostate, and endometrium cancer (6, 38, 39). KAT8 acetylates H4K16 and promotes *Atg* gene transcription (16). Higher levels of H4K16ac promote neuronal autophagy (40). However, the expression and function of KAT8 are different in different biological processes and cell types. KAT8 is also required for embryonic development in *D. melanogaster* and mammals and promotes embryonic stem cell proliferation (41). Many studies have shown that the function of KAT8 and the status of H4K16ac depends on the cell and tissue types (26). We found that KAT8 promoted *Atg* gene transcription and induced larval midgut autophagy under 20E regulation. The function of KAT8 distributing in adult midgut needs further study.

The insect midgut performs remodeling (42). The larval midgut is completely degraded sequentially by autophagy and apoptosis in insects. 20E induces a calcium increase to activate the protease calpain to cleave ATG5 to switch autophagy to apoptosis (15). Autophagy also induces the maturation of cathepsin D, which in turn cleaves caspase-3 to promote apoptosis in the *H. armigera* midgut during metamorphosis (10). Numerous studies have shown that the appearance of ATG8-II is a marker of autophagy (30). This study revealed that 20E upregulated KAT8 expression, which increased H4K16ac level to promote ATG8 expression for autophagy, a basis for apoptosis in the larval midgut during metamorphosis.

FOXO recruits KAT8 to the FOXO-binding region to upregulate Atg *gene transcription*

The autophagy process involves the participation of more than 30 *Atg* genes (43), and KAT8 acetylates H4K16 and promotes *Atg* gene transcription (16). Some studies shown that KAT8-mediated H4K16ac is enriched in gene body rather than promoters, and its acetylation of H4K5 and H4K8 is localized onto promoters and enhancers (34). Some study also shown that KAT8 could regulate the level of H4K16ac in the promoter region to promote profibrotic genes expression in mammals (44). And our study showed that KAT8 increased the level of H4K16ac in the promoter region to promote *Atg8* transcription. However, little is known about the mechanism by which KAT8 specifically regulates histone acetylation in DNA for *Atg* gene expression. Recruitment of HATs to chromatin usually requires a protein transcription factor (45). FOXO is evolutionarily conserved and involved in regulating the transcription of genes involved in a variety of life activities. Many studies have shown that FOXO is associated with autophagy in various cell types from vertebrates to invertebrates (46, 47). FOXO is involved in regulating neuronal autophagy in mice (48) and muscle autophagy in *D. melanogaster* (49). FOXO promotes the transcription of autophagy-related genes, such as *Atg1*, *Atg4*, *Atg6*, *Atg8*, and *Atg12* (18–20). We found FOXOBEs in the promoters of *Atg1*, *Atg4*, *Atg6*, *Atg8*, and *Atg12* and confirmed that FOXO increased the expression of ATG8 by recruiting KAT8 to its promoter to enable gene transcription. In our study, we confirmed that it was FOXO recruited KAT8 to FOXO-binding region and induced H4K16ac to promote the transcription of *Atg8* for autophagy.

KAT8 mediated the acetylation of FOXO and enhances its transcriptional activity

KAT8 can acetylate non-histone, such as P53. KAT8 acetylated P53 at K120 to promote proapoptotic target genes expression and thus induces apoptosis (4). KAT8 interacts with histone demethylase LSD1 and induces its acetylation, thereby suppresses tumor invasion (50). In addition, KAT8 acetylates the transcription factor interferon regulatory factor 3 and plays a crucial role in the suppression of antiviral innate immunity (51). In our study, we found KAT8 also acetylates FOXO. FOXO was acetylated during metamorphosis and 20E promoted FOXO acetylation. FOXO is in an acetylation status in nucleus. This indicated that the acetylation modification of FOXO is crucial for its function during metamorphosis. Previous study has showed that 20E promotes FOXO nuclear translocation by inhibiting its phosphorylation (12). In mammals, the acetylation of FOXO is usually catalyzed by CBP at lysine 242, 245, and 262 (22, 52). And the acetylation at lysine 242 and 245 is associated with its nuclear translocation and activation (53). The acetylation modification activates FOXO3a and FOXO1 transcriptional activity in mammals (54, 55). Histone deacetylase HDAC3 deacetylates FOXO3, which repressed the transcription of its target genes (56). Here, we reported that KAT8 can acetylate FOXO and the acetylation site was at lysine 169, 180, and 183. The acetylation at lysine 180 and 183 was crucial for its function in promoting gene transcription and autophagy, which was a very exciting result.

20E via *FOXO upregulated the expression of KAT8*

In human endometrial carcinoma tissues, the expression of KAT8 is increased with stimulation by estrogen via its receptor (57), but the transcription factor is unclear. We revealed that

FOXO promoted *Kat8* transcription under the regulation of 20E. FOXO is a member of the forkhead transcription factor family that regulates the transcription of multiple genes (58). FOXO also performs various functions in different cellular processes (32), including promoting autophagy in mice muscle (59) and regulating cellular differentiation in *D. melanogaster* (60). Previous research shows that FOXO is highly expressed in the midgut during metamorphosis and promotes the expression of metamorphosis-related genes to start molting, and 20E promotes FOXO expression via EcR and USP (12). In the present study, we found a FOXOBE in the *Kat8* promoter and confirmed that FOXO directly promoted *Kat8* transcription by binding with the FOXOBE on *Kat8* promoter under 20E stimulation. This was an important discovery for understanding the upstream regulation of *Kat8* transcription.

Conclusion

We revealed that FOXO upregulated the expression of KAT8 under 20E regulation, and KAT8 acetylated FOXO in a feedback way to enhance its transcription activity. Acetylation was essential for the function of FOXO in promoting autophagy. FOXO recruited KAT8 to the FOXO-binding element in the promoter region of *Atg8*, where the KAT8 catalyzed histone H4 acetylation nearby to make the DNA accessible to promote *Atg8* transcription for autophagy under 20E regulation. Therefore, FOXO utilizes KAT8 to promote *Atgs* transcription for autophagy (Fig. 9).

Experimental procedures

Experimental insects and HaEpi cells

H. armigera were purchased from Keyun Biology on Taobao. We cultured them in our laboratory at 27 ± 1 °C with a cycle of 14 h in the dark and 10 h in the light and fed them with an artificial diet which was described previously (61). The HaEpi cell line was established from the *H. armigera* epidermis, which was previously well characterized (28). The cells were cultured in tissue culture flasks at 27 °C with Grace's insect cell culture medium containing 10% fetal bovine serum (Gibco). Cell lines were free from *mycoplasma* contamination for all experiments. We observed the cells using an Olympus BX51 (Olympus Optical Co) fluorescence microscope and photographed them at 20 magnification using DP Controler software.

Cloning and sequence analysis of KAT8

One KAT8 was found in the genome of *H. armigera* using KAT8 from *B. mori*, *Homo sapiens*, *D. melanogaster*, *A. aegypti*, and *M. musculus* as query sequences. Sequence analysis with DNAMAN software showed that KAT8 had high similarity with other species (Fig. S11).

Preparation of a polyclonal antibody against KAT8 and FOXO

The selected sequence of KAT8 (1–174 aa) or FOXO (27–307 aa) was amplified with the primer KAT8-exF/R or

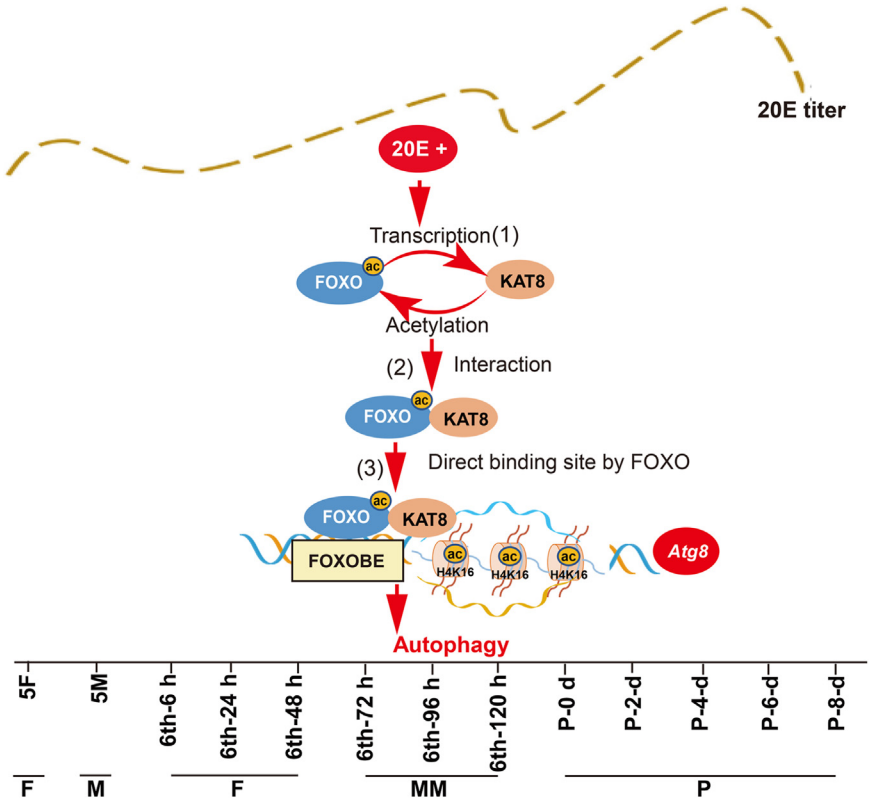

Figure 9. A diagram showing the proposed mechanism by which KAT8 specifically acetylates histone H4K16 in the promotor region of *Atg8* by 20E regulation. 20E *via* FOXO promoted the expression of KAT8 (1). KAT8 interacted and acetylated FOXO (2). FOXO recruited KAT8 to the FOXO-binding region in the promoter region of *Atg8*, where the KAT8 catalyzed histone H4 acetylation to make the DNA accessible for *Atg8* transcription thus for autophagy (3). ATG8, autophagy-related gene 8; FOXO, forkhead box O.

FOXO-exF/R (Table S1) and was inserted into the plasmid pet30a (+). Then the plasmid was transformed in *E. coli* (BL21-DE) and expressed in inclusion bodies. KAT8-His and FOXO-His were purified and used as an antigen. Rabbits were immunized with the purified antigen to obtain rabbit polyclonal antibodies. The molecular weight of KAT8 (1–174 aa) fragment antigen plus His-tag was 36 kDa (Fig. S12*A*). The molecular weight of FOXO (27–307 aa) fragment antigen plus His-tag was about 46 kDa (Fig. S12*B*). The molecular weight recognized by anti-FOXO antibodies is higher than theoretic molecular weight. We identified it and confirmed it and recognized FOXO overexerted in *E. coli* and HaEpi cells, and the increased molecular weight than the theoretic weight was caused by the amino acid sequence of FOXO (Fig. S13). The proteins were used to produce rabbit polyclonal antibodies according to a method described previously (62).

Western blot

For the tissue or cell total protein extraction, 40 mM Tris–HCl or radioimmunoprecipitation assay (RIPA) lysis buffer was used as a lysate, and the protease inhibitor phenylmethanesulfonyl fluoride was added at a ratio of 1:100 to fully extract the worm tissue. After completely grinding the tissue, the homogenate was centrifuged at 10,000 g at 4 °C for 10 min. The total protein was measured by Bradford's method. Next, 50 μg of the protein sample was subjected to 7.5 to 15% sodium dodecyl-sulfate PAGE and transferred to nitrocellulose membranes. The membranes were incubated in blocking buffer (5% fat-free powdered milk in TBST (10 mM Tris–HCl, 150 mM NaCl, 0.02% Tween, pH 7.5)) for 1 h at room temperature. The primary antibody was diluted with blocking buffer and incubated with the membranes overnight at 4 °C. The membrane was washed with TBST twice and incubated with secondary antibody diluted 1:7000. The membrane was immersed in High-sig ECL Western Blotting Substrate (Tanon Science & Technology) and the bands were detected using the ECL luminescence method.

Immunohistochemistry

The midgut was fixed with 4% paraformaldehyde overnight, then sent to a company (Servicebio) for HE staining and for immunofluorescence localization. The pre-serum and anti-KAT8 serum concentration was 1:50. The secondary antibody was Cy3-conjugated goat anti-rabbit IgG (H+L) (1:200, GB21303, Servicebio).

RNAi in larvae

We designed interference primers with an added T7 promoter, which are shown in Table S1. The dsRNA was synthesized with a MEGAscript RNAi kit (Thermo Fisher Scientific). The dsRNA was diluted to a concentration of 400 ng/μl with aseptic PBS. We injected 5 μl of dsRNA into the sixth instar 6 h larvae. About 24 h after the first injection, 5 μl of dsRNA was injected a second time and repeated, for a total of three injections. The same amount of *dsGFP* was injected as a control. Total RNA or protein was extracted at 24 h after the last injection to measure the efficiency of RNAi. The tissues used for morphology and HE staining were obtained 24 h, 72 h, and 96 h after the third injection. Samples for other data analysis were obtained 72 h after the first injection.

qRT-PCR analysis

After extraction of RNA, cDNA was synthesized using a reverse transcription kit (Tiangen). A 2× SYBR RT-PCR premixture was used to perform qRT-PCR, and the primers are listed in Table S1. The relative expression of the target gene was quantified using *H. armigera* β-actin. Each experiment was repeated three times, with three parallel experiments each time. The $2^{-\Delta\Delta CT}$ method was used to analyze the data (63).

Hormonal regulation of KAT8

We stored 20E at a concentration of 20 mM, which was diluted with DMSO. Then the 20E was diluted with PBS to a concentration of 100 ng/μl. Next, 100, 200, 300, or 500 ng of 20E was injected into the sixth instar 6 h larva and were harvested after 6 h, and 500 ng of 20E was injected into the larvae and harvested at 1, 3, 6, or 12 h. The equivalent volume of DMSO was injected as a control. The total mRNA was extracted for qRT-PCR to detect the mRNA level of *Kat8*.

Overexpression of KAT8 in HaEpi cells

The ORFs of *Kat8* were amplified using overexpression primers (Table S1), and the PCR product was inserted into the pIEx-4-GFP-His vector fused with GFP and a His-tag. All recombinant plasmids in the experiments contained a His tag. Then, 5 μg of recombinant plasmids were transfected into HaEpi cells using the Quick Shuttle-enhanced transfection reagent (Biodragon Immunotech). About 72 h after transfection, we extracted total cellular protein for western blotting or other experiments.

ChIP assay

The FOXO-GFP or KAT8-GFP plasmid was transfected into HaEpi cells for 72 h and then treated with 5 μM 20E for 6 h. DMSO treatment was used as a control. Then cells were treated with the ChIP Assay kit (Beyotime Biotechnology, P2078). Cells were incubated with formaldehyde at 37 °C for 10 min to cross-link DNA and proteins. Then cells were treated with the ChIP Assay kit (Beyotime Biotechnology, P2078). Then, a glycine solution was added to the cells at room temperature for 5 min. Cells were collected by centrifugation after washing twice with ice-cold PBS. The cells were suspended in 400 μl of SDS lysis buffer and then sonicated. ChIP dilution buffer and protein A + G resin was added to the supernatant and incubated at 4 °C for 1 h. After centrifugation, one aliquot of supernatant was used as an input sample for qRT-PCR, and the remaining supernatant was incubated with the anti-GFP antibody (with FOXO-GFP overexpression) and anti-H4K16ac antibodies (with KAT8-GFP overexpression) and mouse or rabbit control IgG as a negative control. Then, 60 μl of protein A + G resin was added the solution after 3 h, and the solution was incubated at 4 °C overnight. The complex

was washed with a low-salt wash buffer, high-salt wash buffer, LiCl wash buffer, TE buffer, and elution buffer sequentially. RNase A and proteinase K were added to the DNA and protein complexes to de-crosslink at 65 °C overnight. The DNA was extracted and analyzed with qRT-PCR using primers shown in Table S1.

Luciferase activity assay

A luciferase reporter gene detection kit (US Everbright Inc) was used for the following assay. Seventy-two hours post transfection, the medium was removed and cells were washed with PBS twice, then 1 × lysis buffer diluted with sterile water was added. The culture plate was shaken on a micro-shaker at room temperature for 15 min to fully lyse the cells. The lysate was collected and the supernatant was transferred to a new EP tube. A Enspire 2300 microplate spectrometer was used to measure the sample luciferase activity based on relative light units (RLUs) by adding 100 μl of 0.2 mg/ml firefly luciferase detection solution to each 100 μl sample. Then, 100 μl of 1×coelenterazine working solution was added to each sample and the RLU was measured. The RLU value of the firefly luciferase assay was divided by the RLU value of the Renilla luciferase assay. A comparison of the differences in the degree of activation of the reporter gene plasmids was based on ratios.

Electrophoretic mobility shift assay

We extracted nuclear protein from HaEpi cells expressing FOXO using a nuclear protein extraction kit. DMSO or 20E (5 μM) was added into medium for 6 h, and nuclear protein was extracted according to the instruction. Biotin-labeled probes (sense 5′-GCTGATTGATTAACTA-TGATCAAAGTGTTTATTGATCTTAT-3′ and antisense 5′-ATAAGATCAATAAA-CAC-TTTGATCATAGTTAATCAATCAGC-3′) used in EMSA from the FOXOBE fragment of *Kat8* (sense 5′-GCTGATTGATTAACTATGATCAAAGTGCATGTTGATCTTAT-3′ and antisense 5′- ATAAGATCAACATGCACTTTGATCA-TAGTTAATCAATCAGC-3′) were mutation probe (produced by Sangon Biotech company). The probes were dissolved in the annealing buffer (pH 7.5, 50 mM NaCI, 10 mM Tris, 1 mM EDTA) and heated at 95 °C for 10 min, then slowly cooled to room temperature. The biotin-labeled probes (100 fmol) were incubated with nuclear protein (about 15 μg) in EMSA/Gel-Shift binding buffer for 15 min. An antibody for His (1.5 μl) was added to the binding mixture in the super shift experiment. A 100-fold amount of unlabeled probe was added for competition experiments. One microliter of EMSA/Gel-Shift loading buffer was added into each reaction and then run on a 6.5% polyacrylamide gel at 80 V for 90 min in 0.5 × TBE buffer. Then transfer it onto PVDF membrane use 380 mA constant flow mode for 40 min. The DNA oligomers were crosslinked by UV to the membrane for 20 min. The membrane was blocking in blocking buffer (Beyotime Biotechnology) for 30 min. HRP-Streptavidin was added into new blocking buffer by 1:3000 and incubated the membrane with mixture buffer for 40 min. Then the labeled probe was detected by chemiluminescent method.

Co-immunoprecipitation

For the KAT8 and FOXO *in vitro* Co-IP assay, KAT8-GFP and FOXO-RFP were cotransfected into HaEpi cells for 72 h, followed by treatment of cells with 20E or DMSO for 6 h. Cells were lysed with 500 μl of RIPA lysis buffer for 30 min and harvested by centrifugation at 12,000 g for 15 min at 4 °C. Then, 50 μl of protein A was added to the supernatant and samples were shaken for 1 h at 4 °C to reduce nonspecific binding. Then, 40 μl of the supernatant was used as an input. Anti-GFP/IgG antibodies were added into the remaining supernatant and incubated overnight at 4 °C. Then 50 μl of protein A was added, and samples were incubated for 4 h and washed three times with lysis buffer. The resin was resuspended with 40 μl of lysis buffer and used for Western blot assays. For the KAT8 and FOXO *in vivo* Co-IP assay, anti-KAT8 and IgG antibodies were added to CNBr-activated Sepharose 4B resin and incubated overnight at 4 °C. Then the resin was washed five times with binding buffer (0.1 M NaHCO3, 0.5 M NaCl, pH 8.3) and blocked for 1 h with blocking buffer (0.1 M Tris–HCl, pH 8.0). Then the resin was washed with the following solutions sequentially: sodium acetate buffer (0.1 M NaAc, 0.5 M NaCl, pH 8.3). Tris buffer (0.1 M Tris–HCl, 0.5 M NaCl, pH 8.0), and wash buffer (0.1 M Tris–HCl, 0.1 M NaCl, pH 8.0). The tissue was ground thoroughly with RIPA lysis buffer and shaken gently at 4 °C for 30 min. The supernatant was harvested by centrifugation at 12,000*g* for 15 min at 4 °C and incubated with CNBr beads overnight. The beads were washed three times with wash buffer and the bound complex was eluted with buffer (0.1 M glycine, pH 2.5) and used in Western blot assays.

In vitro *GST pull-down assay*

FOXO-GST was generated by cloning *H. armigera* protein ORF into pGEX-4T-1 vector using BamH I and SalI restriction sites. The following experiments were based on previous experimental methods (64). GST and FOXO-GST was purified from *E. coli* and incubated with cell lysates overexpressing KAT8-GFP at 4 °C for 4 h. Then 30 μl glutathione-sepharose 4B beads was added into the mixture and incubated for 2 h and washed three times with PBS after centrifugation of 1000*g* at 4 °C. The beads were washed with elution buffer (150 mM Nacl, 50 mM Tris–Hcl, 10 mM Glutathione, pH 8.0). And the supernatant was used for Western blot assay.

FOXO acetylation assay

Midgut tissue was collected after *dsKat8* or 20E injection or from different period (6th-24 h and 6th-96 h). After completely grinding the tissue with 500 μl of RIPA lysis buffer, the homogenate was centrifuged at 12,000*g* at 4 °C for 15 min. For FOXO acetylation analysis on cells, the GFP or KAT8-GFP plasmid was transfected into HaEpi cells for 72 h. Cells were lysed with 500 μl of RIPA lysis buffer for 30 min and harvested by centrifugation at 12,000*g* for 15 min at 4 °C. Then, 50 μl of protein A was added to the supernatant and samples were shaken for 1 h at 4 °C to reduce nonspecific binding. Forty microliters of the supernatant was used as an input. Anti-

FOXO antibodies were added into the remaining supernatant and incubated overnight at 4 °C. Then 50 μl of protein A was added, and samples were incubated for 4 h and washed three times with lysis buffer. The resin was resuspended with 40 μl of lysis buffer and used for Western blot assays. FOXO was used as a protein quantity control. After homogenization, FOXO acetylation was detected with anti-acetyl lysine antibody.

FOXO-GFP acetylation assay

Cells were collected after transfected with FOXO-GFP, FOXO-K169R-GFP, FOXO-K180R-GFP, and FOXO-K183R-GFP for 72 h with 20E treatment. Cells were lysed with RIPA lysis buffer for 30 min and harvested by centrifugation at 12,000*g* for 20 min at 4 °C. The His-binding resin was washed with lysis buffer for three times and added, and the samples were shaken for 1 h. Then wash the resin with wash buffer for 3 to 4 times. The resin was resuspended with 40 μl of elution buffer and used for Western blot assays. FOXO-GFP was used as a protein quantity control. After homogenization, FOXO acetylation was detected with anti-acetyl lysine antibody.

In vitro *acetylation assay*

FOXO-GST was purified from *E. coli* and KAT8-GFP (contains His tag) was purified from HaEpi cells. They were incubated together in HAT assay buffer (10% glycerol, 50 mM Tris–HCl, 1 mM DTT, 0.1 mM EDTA, pH 8.0) with 1 mM acetyl-coenzyme A at 30 °C for 3 h. The acetylation on FOXO was analyzed by Western blot.

Quantification and statistical analysis

All results were repeated at least three times and analyzed using Student's *t* test for the comparison of two groups of data or one-way Anova for multiple comparisons. GraphPad 8 software (https://www.graphpad.com) were used for data analysis and graphing. The error bars represent the SD of three independent experiments. An asterisk indicates a significant difference ($^{*}p < 0.05$, $^{**}p < 0.01$, and $^{***}p < 0.001$). In the ANOVA analysis, different letters indicate significant differences ($p < 0.05$). The protein bands analysis of the Western blot was quantified with ImageJ software (National Institutes of Health, http//imagej.nih.gov/ij/download.html). The three points on the statistical chart corresponding to each Western blot represent the results of threefold repetition data and are shown as means ± SD.

The antibodies used in this study

The following antibodies were used in our study: rabbit anti-H3 (1:3000, 1768-1-AP, RRID: AB_2716755, Proteintech, America), rabbit-anti-H4K16ac (1:1000 for Western blot and 1:100 for ChIP and Co-IP, PTM-122, PTM Biolab), rabbit-anti-H4K5ac (1:2000 for Western blot and 1:100 for ChIP, PTM-119, PTM Biolab), rabbit-anti-H4K8ac (1:2000 for Western blot and 1:100 for ChIP, PTM-120, PTM Biolab), rabbit anti-actin (1:3000, AC026, RRID: AB_2768234, ABclonal Technology), rabbit anti-acetyl Lysine Antibody (1:2000 for Western blot and 1:200 for Co-IP, ICP0380, Immunechem), rabbit anti-IgG (1:3000 for Western blot and 1:200 for Co-IP and ChIP, AS061, ABclonal Technology), mouse anti-IgG (1:200 for ChIP, AC011, ABclonal Technology), mouse anti-GFP (1:3000 for Western blot and 1:200 for Co-IP and ChIP, AE012, RRID: AB_2770402, ABclonal Technology), and mouse anti-RFP (1:3000 for Western blot and 1:200 for Co-IP, AE020, RRID: AB_2770409, ABclonal Technology). The antibodies against *H. armigera* ATG8, KAT8, and FOXO were prepared in our laboratory. The dilution of anti-KAT8 and FOXO for Co-IP was 1:60 and for Western blot was 1:500.

Ethics statement

The antibody preparation in rabbits was in accordance with protocols approved by the Animal Care & Welfare Committee, Shandong University School of Life Sciences (SYDWLL-2021-54).

Data availability

All data are contained within the article. This article contains supporting information. Any additional information required to reanalyze the data reported in this paper is available from the lead contact Xiao-Fan Zhao (xfzhao@sdu.edu.cn) upon request.

Supporting information—This article contains supporting information.

Acknowledgments—We thank Hai-Yan Sui, Zhao-Yuan Cui, Xiang-Mei Ren, Jing-Yao Qu, and Yan Wang of the Core Facilities for Life and Environmental Sciences and State Key Laboratory of Microbial Technology of Shandong University for operation and analysis of the high-speed refrigerated centrifuge CR21G III, Tecan microplate reader spectrophotometer and qRT-PCR instrument. This work was supported by the National Natural Science Foundation of China (Grant Nos. 32330011 and 32270507).

Author contributions—T.-W. L. and Y.-M. Z. investigation; T.-W. L. writing–original draft; K.-Y. J., J.-X. W., and X.-F. Z. methodology; J.-X. W. and X.-F. Z. writing–review and editing.

Conflict of interest—The authors declare that they have no conflicts of interest with the contents of this article.

Abbreviations—The abbreviations used are: 20E, 20-hydroxyecdysone; ATG8, autophagy-related gene 8; ChIP, chromatin immunoprecipitation; Co-IP, co-immunoprecipitation; DMSO, dimethyl sulfoxide; FOXO, forkhead box O; FOXOBE, FOXO-binding element; H4K16ac, acetylation of histone H4 at K16; HaEpi, H. armigera epidermal cell line; HAT, histone acetyltransferase; KAT8, histone acetyltransferase 8; LC3, microtubule-associated protein 1 light chain 3-phosphatidylethanolamine; MM, metamorphic stage; qRT-PCR, quantitative real-time polymerase chain reaction; RIPA, radioimmunoprecipitation assay; RLU, relative light unit.

References

1. Kuo, M. H., and Allis, C. D. (1998) Roles of histone acetyltransferases and deacetylases in gene regulation. *BioEssays* **20**, 615–626

2. Trisciuoglio, D., Di Martile, M., and Del Bufalo, D. (2018) Emerging role of histone acetyltransferase in stem cells and cancer. *Stem Cells Int.* **2018**, 8908751
3. Neal, K. C., Pannuti, A., Smith, E. R., and Lucchesi, J. C. (2000) A new human member of the MYST family of histone acetyl transferases with high sequence similarity to *Drosophila* MOF. *Biochim. Biophys. Acta* **1490**, 170–174
4. Sykes, S. M., Mellert, H. S., Holbert, M. A., Li, K., Marmorstein, R., Lane, W. S., *et al.* (2006) Acetylation of the p53 DNA-binding domain regulates apoptosis induction. *Mol. Cell* **24**, 841–851
5. Belote, J. M., and Lucchesi, J. C. (1980) Male-specific lethal mutations of *Drosophila melanogaster*. *Genetics* **96**, 165–186
6. Su, J., Wang, F., Cai, Y., and Jin, J. (2016) The functional analysis of histone acetyltransferase MOF in tumorigenesis. *Int. J. Mol. Sci.* **17**, 99
7. Sheikh, B. N., Bechtel-Walz, W., Lucci, J., Karpiuk, O., Hild, I., Hartleben, B., *et al.* (2016) MOF maintains transcriptional programs regulating cellular stress response. *Oncogene* **35**, 2698–2710
8. Fullgrabe, J., and Klionsky, D. J. (2014) The return of the nucleus: transcriptional and epigenetic control of autophagy. *Nat. Rev. Mol. Cell Biol.* **15**, 65–74
9. Fullgrabe, J., Lynch-Day, M. A., Heldring, N., Li, W., Struijk, R. B., Ma, Q., *et al.* (2013) The histone H4 lysine 16 acetyltransferase hMOF regulates the outcome of autophagy. *Nature* **500**, 468–471
10. Di, Y. Q., Han, X. L., Kang, X. L., Wang, D., Chen, C. H., Wang, J. X., *et al.* (2021) Autophagy triggers CTSD (cathepsin D) maturation and localization inside cells to promote apoptosis. *Autophagy* **17**, 1170–1192
11. Riddiford, L. M. (1993) Hormone receptors and the regulation of insect metamorphosis. *Receptor* **3**(3), 203–209
12. Cai, M. J., Zhao, W. L., Jing, Y. P., Song, Q., Zhang, X. Q., Wang, J. X., *et al.* (2016) 20-Hydroxyecdysone activates forkhead box O to promote proteolysis during *Helicoverpa armigera* molting. *Development* **143**, 1005–1015
13. Yin, V. P., and Thummel, C. S. (2004) A balance between the diap1 death inhibitor and reaper and hid death inducers controls steroid-triggered cell death in *Drosophila*. *Proc. Natl. Acad. Sci. U. S. A.* **101**, 8022–8027
14. Liu, H., Wang, J., and Li, S. (2014) E93 predominantly transduces 20-hydroxyecdysone signaling to induce autophagy and caspase activity in *Drosophila* fat body. *Insect Biochem. Mol. Biol.* **45**, 30–39
15. Li, Y. B., Li, X. R., Yang, T., Wang, J. X., and Zhao, X. F. (2016) The steroid hormone 20-hydroxyecdysone promotes switching from autophagy to apoptosis by increasing intracellular calcium levels. *Insect Biochem. Mol. Biol.* **79**, 73–86
16. Lapierre, L. R., Kumsta, C., Sandri, M., Ballabio, A., and Hansen, M. (2015) Transcriptional and epigenetic regulation of autophagy in aging. *Autophagy* **11**, 867–880
17. Xu, Y., and Wan, W. (2022) Acetylation in the regulation of autophagy. *Autophagy* **10**, 1–9
18. Sengupta, A., Molkentin, J. D., and Yutzey, K. E. (2009) FoxO transcription factors promote autophagy in cardiomyocytes. *J. Biol. Chem.* **284**, 28319–28331
19. Mammucari, C., Schiaffino, S., and Sandri, M. (2008) Downstream of Akt: FoxO3 and mTOR in the regulation of autophagy in skeletal muscle. *Autophagy* **4**, 524–526
20. Mammucari, C., Milan, G., Romanello, V., Masiero, E., Rudolf, R., Del Piccolo, P., *et al.* (2007) FoxO3 controls autophagy in skeletal muscle *in vivo*. *Cell Metab.* **6**, 458–471
21. Wang, Z., Yu, T., and Huang, P. (2016) Post-translational modifications of FOXO family proteins (Review). *Mol. Med. Rep.* **14**, 4931–4941
22. Ng, F., and Tang, B. L. (2013) Sirtuins' modulation of autophagy. *J. Cell Physiol.* **228**, 2262–2270
23. Bhol, C. S., Panigrahi, D. P., Praharaj, P. P., Mahapatra, K. K., Patra, S., Mishra, S. R., *et al.* (2020) Epigenetic modifications of autophagy in cancer and cancer therapeutics. *Semin. Cancer Biol.* **66**, 22–33
24. Gu, W., Szauter, P., and Lucchesi, J. C. (1998) Targeting of MOF, a putative histone acetyl transferase, to the X chromosome of *Drosophila melanogaster*. *Dev. Genet.* **22**, 56–64
25. Fullgrabe, J., Klionsky, D. J., and Joseph, B. (2013) Histone post-translational modifications regulate autophagy flux and outcome. *Autophagy* **9**, 1621–1623
26. Sheikh, B. N., and Akhtar, A. (2019) The many lives of KATs — detectors, integrators and modulators of the cellular environment. *Nat. Rev. Genet.* **20**, 7–23
27. Wang, J. L., Jiang, X. J., Wang, Q., Hou, L. J., Xu, D. W., Wang, J. X., *et al.* (2007) Identification and expression profile of a putative basement membrane protein gene in the midgut of *Helicoverpa armigera*. *BMC Dev. Biol.* **7**, 76
28. Shao, H. L., Zheng, W. W., Liu, P. C., Wang, Q., Wang, J. X., and Zhao, X. F. (2008) Establishment of a new cell line from lepidopteran epidermis and hormonal regulation on the genes. *PLoS One* **3**, e3127
29. Liu, C. Y., Liu, W., Zhao, W. L., Wang, J. X., and Zhao, X. F. (2013) Upregulation of the expression of prodeath serine/threonine protein kinase for programmed cell death by steroid hormone 20-hydroxyecdysone. *Apoptosis* **18**, 171–187
30. Klionsky, D. J., Abdelmohsen, K., Abe, A., Abel, S., Abeliovich, H., Abildgaard, M. H., *et al.* (2016) Guidelines for the use and interpretation of assays for monitoring autophagy. *Autophagy* **12**, 1–222
31. Cheng, Z. (2019) The FoxO-autophagy Axis in Health and disease. *Trends Endocrinol. Metab.* **30**, 658–671
32. Eijkelenboom, A., and Burgering, B. M. (2013) FOXOs: signalling integrators for homeostasis maintenance. *Nat. Rev. Mol. Cell Biol.* **14**, 83–97
33. Barthel, A., Schmoll, D., and Unterman, T. G. (2005) FoxO proteins in insulin action and metabolism. *Trends Endocrinol. Metab.* **16**, 183–189
34. Radzisheuskaya, A., Shliaha, P. V., Grinev, V. V., Shlyueva, D., Damhofer, H., Koche, R., *et al.* (2021) Complex-dependent histone acetyltransferase activity of KAT8 determines its role in transcription and cellular homeostasis. *Mol. Cell* **81**, 1749–1765.e1748
35. Chen, Q. Y., Costa, M., and Sun, H. (2015) Structure and function of histone acetyltransferase MOF. *AIMS Biophys.* **2**, 555–569
36. Pushpavalli, S. N., Sarkar, A., Ramaiah, M. J., Koteswara, R. G., Bag, I., Bhadra, U., *et al.* (2016) *Drosophila* MOF regulates DIAP1 and induces apoptosis in a JNK dependent pathway. *Apoptosis* **21**, 269–282
37. Li, T., Lu, D., Yao, C. C., Li, T. T., Dong, H., Li, Z., *et al.* (2022) Kansl1 haploinsufficiency impairs autophagosomelysosome fusion and links autophagic dysfunction with Koolen-de Vries syndrome in mice. *Nat. Commun.* **13**, 931
38. Kim, J. Y., Yu, J., Abdulkadir, S. A., and Chakravarti, D. (2016) KAT8 regulates androgen signaling in prostate cancer cells. *Mol. Endocrinol.* **30**, 925–936
39. Fraga, M. F., Ballestar, E., Villar-Garea, A., Boix-Chornet, M., Espada, J., Schotta, G., *et al.* (2005) Loss of acetylation at lys16 and trimethylation at Lys20 of histone H4 is a common hallmark of human cancer. *Nat. Genet.* **37**, 391–400
40. Lingling, D., Miaomiao, Q., Yili, L., Hongyun, H., and Yihao, D. (2022) Attenuation of histone H4 lysine 16 acetylation (H4K16ac) elicits a neuroprotection against ischemic stroke by alleviating the autophagic/lysosomal dysfunction in neurons at the penumbra. *Brain Res. Bull* **184**, 24–33
41. Singh, M., Bacoll, a A., Chaudhary, S., Hunt, C. R., Pandita, S., Chauhan, R.,., *et al.* (2020) Histone acetyltransferase MOF orchestrates outcomes at the crossroad of oncogenesis, DNA damage response, proliferation, and stem cell development. *Mol. Cell Biol.* **40**, e00232-00220
42. Zhao, X. F. (2020) G protein-coupled receptors function as cell membrane receptors for the steroid hormone 20-hydroxyecdysone. *Cell Commun. Signal.* **18**, 146
43. Mizushima, N. (2007) Autophagy: process and function. *Genes Dev.* **21**, 2861–2873
44. Zhang, X., Liu, H., Zhou, J. Q., Krick, S., Barnes, J. W., Thannickal, V. J., *et al.* (2022) Modulation of H4K16Ac levels reduces pro-fibrotic gene expression and mitigates lung fibrosis in aged mice. *Theranostics* **12**, 530–541
45. Voss, A. K., and Thomas, T. (2018) Histone lysine and genomic targets of histone acetyltransferases in mammals. *Bioessays* **40**, e1800078
46. Webb, A. E., and Brunet, A. (2014) FOXO transcription factors: key regulators of cellular quality control. *Trends Biochem. Sci.* **39**, 159–169
47. Zhao, J., Brault, J. J., Schild, A., and Goldberg, A. L. (2008) Coordinate activation of autophagy and the proteasome pathway by FoxO transcription factor. *Autophagy* **4**, 378–380

48. Xu, P., Das, M., Reilly, J., and Davis, R. J. (2011) JNK regulates FoxO-dependent autophagy in neurons. *Genes Dev.* **25**, 310–322
49. Demontis, F., and Perrimon, N. (2010) FOXO/4E-BP signaling in *Drosophila* muscles regulates organism-wide proteostasis during aging. *Cell* **143**, 813–825
50. Luo, H., Shenoy, A. K., Li, X., Jin, Y., Jin, L., Cai, Q., *et al.* (2016) MOF acetylates the histone demethylase LSD1 to suppress epithelial-to-mesenchymal transition. *Cell Rep.* **15**, 2665–2678
51. Huai, W., Liu, X., Wang, C., Zhang, Y., Chen, X., Chen, X., *et al.* (2019) KAT8 selectively inhibits antiviral immunity by acetylating IRF3. *J. Exp. Med.* **216**, 772–785
52. van der Heide, L. P., and Smidt, M. P. (2005) Regulation of FoxO activity by CBP/p300-mediated acetylation. *Trends Biochem. Sci.* **30**, 81–86
53. Consolaro, F., Ghaem-Maghami, S., Bortolozzi, R., Zona, S., Khongkow, M., Basso, G., *et al.* (2015) FOXO3a and posttranslational modifications mediate glucocorticoid sensitivity in B-ALL. *Mol. Cancer Res.* **13**, 1578–1590
54. Maria, M., Nullin, D., Madeleine, L., Christopher, K., Delin, C., and Wei, G. (2004) Mammalian SIRT1 represses forkhead transcription factors. *Cell* **116**, 551–563
55. Perrot, V.r., and Rechler, M. M. (2005) The coactivator p300 directly acetylates the forkhead transcription factor Foxo1 and stimulates foxo1-induced transcription. *Mol. Endocrinol.* **19**, 2283–2298
56. Zhang, L., Cai, M., Gong, Z., Zhang, B., Li, Y., Guan, L., *et al.* (2017) Geminin facilitates FoxO3 deacetylation to promote breast cancer cell metastasis. *J. Clin. Invest.* **127**, 2159–2175
57. Qi, Y., Tan, M., Zheng, M., Jin, S., Wang, H., Liu, J., *et al.* (2020) Estrogen/estrogen receptor promotes the proliferation of endometrial carcinoma cells by enhancing hMOF expression. *Jpn. J. Clin. Oncol.* **50**, 241–253
58. Kaufmann, E., and Knöchel, W. (1996) Five years on the wings of fork head. *Mech. Dev.* **57**, 3–20
59. Milan, G., Romanello, V., Pescatore, F., Armani, A., Paik, J. H., and Frasson, L. (2015) Regulation of autophagy and the ubiquitin-proteasome system by the FoxO transcriptional network during muscle atrophy. *Nat. Commun.* **6**, 6670
60. Puig, O., and Mattila, J. (2011) Understanding Forkhead box class O function: lessons from *Drosophila melanogaster*. *Antioxid. Redox Signal.* **14**, 635–647
61. Zhao, X. F., Wang, J. X., and Wang, Y. C. (1998) Purification and characterization of a cysteine proteinase from eggs of the cotton boll worm, *Helicoverpa armigera*. *Insect Biochem. Mol. Biol.* **28**, 259–264
62. Zhao, X.-F., Wang, J.-X., Cai, M.-J., and Liu, W. (2014) In a nongenomic action, steroid hormone 20-hydroxyecdysone induces phosphorylation of cyclin-dependent kinase 10 to promote gene transcription. *Endocrinology* **155**, 1738–1750
63. Liu, M., Udhe-Stone, C., and Goudar, C. T. (2011) Progress curve analysis of qRT-PCR reactions using the logistic growth equation. *Biotechnol. Prog.* **27**, 1407–1414
64. You Z, J. W., Qin, L. Y., Gong, Z., Wan, W., and Li, J. (2019) Requirement for p62 acetylation in the aggregation of ubiquitylated proteins under nutrient stress. *Nat. Commun.* **10**, 5792